Atmos. Chem. Phys. Discuss., 14, 25095–25138, 2014
www.atmos-chem-phys-discuss.net/14/25095/2014/
doi:10.5194/acpd-14-25095-2014

Atmospheric Chemistry and Physics Discussions

Properties and evolution of biomass burning organic aerosol from Canadian boreal forest fires

M. D. Jolleys[1], H. Coe[1], G. McFiggans[1], J. W. Taylor[1], S. J. O'Shea[1], M. Le Breton[1], S. J.-B. Bauguitte[2], S. Moller[3], P. Di Carlo[4,5], E. Aruffo[4,5], P. I. Palmer[6], and J. D. Lee[3]

[1]Centre for Atmospheric Science, School of Earth, Atmospheric and Environmental Science, University of Manchester, Manchester, UK
[2]Facility for Airborne Atmospheric Measurements, Bedford, UK
[3]National Centre for Atmospheric Science (NCAS), Department of Chemistry, University of York, York, UK
[4]Centre of Excellence CETEMPS, University of L'Aquila, L'Aquila, Italy
[5]Department of Physical and Chemical Sciences, University of L'Aquila, L'Aquila, Italy
[6]School of Geosciences, University of Edinburgh, Edinburgh, UK

Received: 4 August 2014 – Accepted: 26 August 2014 – Published: 1 October 2014

Correspondence to: M. D. Jolleys (matthew.jolleys@manchester.ac.uk)

Published by Copernicus Publications on behalf of the European Geosciences Union.

Abstract

Airborne measurements of biomass burning organic aerosol (BBOA) from boreal forest fires reveal highly contrasting properties for plumes of different ages. These measurements, performed using an Aerodyne Research Inc. compact time-of-flight aerosol mass spectrometer (C-ToF-AMS) during the BORTAS (quantifying the impact of BOreal forest fires on Tropospheric oxidants over the Atlantic using Aircraft and Satellites) experiment in the summer of 2011, have been used to derive normalised excess organic aerosol (OA) mass concentrations ($\Delta OA/\Delta CO$), with higher average ratios observed closer to source (0.190 ± 0.010) than in the far-field (0.097 ± 0.002). The difference in $\Delta OA/\Delta CO$ between fresh and aged plumes is influenced by a change in dominant combustion conditions throughout the campaign. Measurements at source sampled largely smouldering fires, while plumes encountered in the far-field originated from fires occurring earlier in the campaign when fire activity had been more intense. Changing combustion conditions also affect the vertical distribution of biomass burning emissions, as aged plumes from more flaming-dominated fires are injected to higher altitudes of up to 6000 m. Proportional contributions of the mass-to-charge ratio (m/z) 60 and 44 peaks in the AMS mass spectra to the total OA mass (denoted f_{60} and f_{44}) are used as tracers for primary and oxidized BBOA, respectively. Given the shorter aging times associated with near-field plumes, f_{44} is lower on average than in more aged, transported plumes. However, high levels of $\Delta O_3/\Delta CO$ and $-\log(NO_x/NO_y)$ close to source indicate that emissions can be subject to very rapid oxidation over short timescales. Conversely, the lofting of plumes into the upper troposphere can lead to the retention of source profiles after transportation over extensive temporal and spatial scales, with f_{60} also higher on average in aged plumes. Evolution of OA composition with aging is comparable to observations of BB tracers in previous studies, revealing a consistent progression from f_{60} to f_{44}. The elevated levels of oxygenation in aged plumes, and their association with lower average $\Delta OA/\Delta CO$, highlight the influence of

ACPD
14, 25095–25138, 2014

OA losses during aging, although there remain considerable uncertainties regarding the role of combustion processes on BBOA production and composition.

1 Introduction

The BORTAS (quantifying the impact of BOReal forest fires on Tropospheric oxidants over the Atlantic using Aircraft and Satellites) campaign was a major international research effort to improve understanding of the properties and evolution of biomass burning (BB) plumes. BB emissions form a major source of atmospheric particulate matter on a global scale, contributing around 90 % of the total primary organic aerosol (OA) (Bond et al., 2004). The radiative effects of atmospheric aerosols represent one of the major sources of uncertainty with regard to influences on climate change (Textor et al., 2006; Forster et al., 2007). Given the prominence of OA in global aerosol budgets (Zhang et al., 2007; Jimenez et al., 2009), limited understanding of BB emissions, and more specifically biomass burning organic aerosol (BBOA), forms an important component of this uncertainty. Improved projection of climate change impacts through global climate model simulation is dependent on more robust parameterisation of the constituent drivers, constrained by direct measurements. Several fundamental aspects of the BBOA lifecycle remain poorly characterised, including the conditions and processes controlling formation, and the effects of transformations occurring during aging (Hallquist et al., 2009). Variability at source has been shown to be extensive, in response to changes in both fuel properties and combustion conditions (McMeeking et al., 2009; Jolleys et al., 2012, 2014). The influence of secondary organic aerosol (SOA) in aging plumes is also particularly unclear. Substantial SOA formation as a result of photochemical processing has been demonstrated in laboratory experiments, increasing OA concentrations by up to a factor of 4 over several hours (Grieshop et al., 2009; Hennigan et al., 2011; Heringa et al., 2011). However, under ambient conditions the importance of SOA addition relative to primary (POA) emissions is more disputable. Despite widespread evidence for the increasing oxygenation of BBOA with

ACPD
14, 25095–25138, 2014

aging (Capes et al., 2008; DeCarlo et al., 2008; Cubison et al., 2011; Jolleys et al., 2012), net mass enhancements are not observed consistently. The underlying causes of this variable SOA contribution, including the implications of initial OA composition, also remain ambiguous and require further refinement.

The BORTAS campaign is described in detail by Palmer et al. (2013), with an overview of measurements used within this analysis given here. BORTAS took place across several regions of Canada between the 12 July and 3 August in both 2010 and 2011, although activity during the 2010 deployment (BORTAS-A) was limited to ground-based measurements at a main ground station located at Dalhousie University in Halifax, Nova Scotia, along with ozonesonde launches from a network of seven sites across central and eastern Canada and supporting satellite observations (Parrington et al., 2012). Airborne measurements were carried out during BORTAS-B in 2011, providing all data contributing towards this study. The UK Facility for Airborne Atmospheric Measurements (FAAM) BAe-146 Atmospheric Research Aircraft (ARA) performed a total of 15 flights, including 11 dedicated science flights between the 15 and 31 July. Research flights primarily originated from Halifax and largely involved surveying areas adjacent to the Gulf of St. Lawrence and the North Atlantic. A predominant source region in northwestern Ontario (approximately 52.5° N, 93.5° W) has been identified for the majority of plumes sampled throughout BORTAS, although more disperse fires were also active in northern Alberta and the Northwest Territories (Palmer et al., 2013; Parrington et al., 2013). As the majority of plumes from fires in this region were encountered at a distance of several thousand kilometres downwind, emissions would have undergone substantial processing prior to sampling, with estimated photochemical ages between 1–11 days. A single flight to the Ontario source region also sampled active fires directly at source, providing a valuable inventory of fresh plume measurements and enabling comparison of emissions in the near and far-field. Tracks of all flights included within this analysis are shown in the Supplement (Fig. S1). Comparison of emissions of different ages is subject to potential contrasts in fire behaviour, given that each set of measurements were obtained at different stages of the campaign. Fire activity within

ACPD
14, 25095–25138, 2014

the region peaked between the 17 and 19 July (Supplement Fig. S2), with emissions from these fires intercepted far downwind. Plumes from active fires within this region were also sampled at source on the 26 July (flight B626), representing the only measurements of fresh plumes from BORTAS. However, by this time fire activity had significantly abated, bringing about a change in combustion conditions to yield smaller, less intense fires more typically dominated by smouldering combustion (O'Shea et al., 2013a). The more intense period of fires earlier in the campaign is expected to involve larger events with a more prominent flaming combustion phase, as indicated by the detection of pronounced smoke plumes at altitudes of up to approximately 7000 m over the North Atlantic (Palmer et al., 2013). As a result, any comparison of fresh and aged plumes during BORTAS must also account for this disparity in source conditions. While such a scenario would reduce the potential to evaluate the continuous evolution of smoke plumes from source into the ambient atmosphere, and prevent direct comparison of near and far-field plumes derived from similar combustion conditions, it also provides a baseline for conditions at source.

2 Background

2.1 Instrumentation and measurements

A wide array of instrumentation performing particulate and gas phase measurements were deployed throughout BORTAS. This study focuses primarily on the analysis of OA mass and composition data obtained from an Aerodyne Research Inc. compact time-of-flight aerosol mass spectrometer (C-ToF-AMS; Drewnick et al., 2005; Canagaratna et al., 2007). The AMS provides highly time-resolved mass concentrations of sub-micron, non-refractory aerosol, and a broad chemical characterisation across a complete range of constituent ion mass-to-charge ratios (m/z). Operation of the AMS, including calibration and necessary correction factors, during aircraft deployment (Bahreini et al., 2003) and specifically onboard the BAe-146 (Crosier et al., 2007;

ACPD
14, 25095–25138, 2014

Morgan et al., 2009; Taylor et al., 2013) have been described in detail. Refractory black carbon (BC) was measured using a Droplet Measurement Technologies single particle soot photometer (SP-2; Schwarz et al., 2006; Taylor et al., 2013). Although analysis of the chemical and optical properties of single BC particles was not performed as part of this study, mass concentrations in smoke plumes, particularly in relation to OA concentrations, were used as a means of evaluating the proportional contributions of different combustion phases. A range of gas phase measurements were undertaken on the BAe-146, including species used as tracers for both primary emissions and photochemical processing. CO mixing ratios were measured with an Aerolaser AL5002 UV fluorescence analyser and O_3 by a Thermo Scientific TEi49C UV photometric analyser as part of the standard complement of instrumentation for BAe-146 science flights. Additional instrumentation included a chemical ionisation mass spectrometer (CIMS; Nowak et al., 2007; Le Breton et al., 2012) providing real-time measurements of HCN, which is widely used as a tracer for BB emissions given that vegetation fires constitute its primary global source (Li et al., 2000; Sinha et al., 2003; Yokelson et al., 2007). NO_x ($NO + NO_2$) and NO_y (NO_x oxidation products, including HNO_3 and N_2O_5) act as important tracers for oxidation in aging plumes, and were measured respectively by an Air Quality Design Inc. chemiluminescence NO_x analyser and by thermal dissociation-laser induced fluorescence (TD-LIF; Di Carlo et al., 2013). The assembly of gas phase measurements used within this analysis was completed by CO_2 mixing ratios from a Los Gatos Research Inc. cavity enhanced absorption spectrometer-based fast greenhouse gas analyser (FGGA; O'Shea et al., 2013b). Aerosol size distributions in the range 20–350 nm were obtained from a scanning mobility particle sizer (SMPS), with integrated distributions over the full size range used as an approximation of particle number concentration.

2.2 Data selection

Data from BORTAS were screened in order to isolate emissions with a biomass burning influence. This was performed using the guidelines proposed by Capes et al. (2008)

ACPD
14, 25095–25138, 2014

and Jolleys et al. (2012) based upon minimum ΔCO (the excess CO concentration above background levels) and number concentrations. A threshold of 0.003 was used for f_{60}, representing the ratio of levoglucosan-like species, which correspond to the m/z 60 peak in the AMS mass spectra (Schneider et al., 2006; Alfarra et al., 2007), to the total OA mass. This threshold is based upon observed background levels of f_{60} in OA emissions from urban and biogenic sources where BB influences are absent (Cubison et al., 2011; Aiken et al., 2009; DeCarlo et al., 2008). Levoglucosan and other anhydrous sugars such as mannosan and galactosan have been shown to be strongly associated with primary BB emissions (Simoneit et al., 1999; Iinuma et al., 2007; Sullivan et al., 2008; Lee et al., 2010). Respective thresholds of 20 ppb and 2000 cm^{-3} were applied for ΔCO and number concentration. Background CO concentrations were calculated for each flight according to the minimum observed concentrations. All data were also averaged to the temporal resolution of the AMS (~ 8 s time step on average) to enable direct comparison of different species. Alternative screening procedures for BB influences have been applied throughout separate analyses of BORTAS data (Palmer et al., 2013). Concentrations of trace gases primarily produced by fire sources, including HCN and CH_3CN, are commonly used as indicators for BB plumes (Li et al., 2000; Yokelson et al., 2007, 2009; Crounse et al., 2009; Akagi et al., 2011). A scheme using a HCN concentration threshold of six times the standard deviation (6σ) has been proposed for BORTAS (Le Breton et al., 2013). However, to ensure consistency with previous assessments of BBOA and facilitate intercomparison of different datasets, a simplified scheme using only OA, CO and number concentration data has been applied here. This approach performs well when compared to other methods, producing similarly strong correlations between HCN and CO for flights B621, B622, B624 and B626 (R^2 = 0.64, 0.52, 0.84 and 0.93) as the 6σ technique (R^2 = 0.83, 0.46, 0.82 and 0.81). These four flights, in addition to B623, were the only flights from which data was used in this analysis, although HCN was not measured during B623, preventing comparison of classification schemes for this flight. Several flights carried out later in the campaign (B628-B630) also measured highly aged plumes with a photochemical

ACPD
14, 25095–25138, 2014

age of up to 11 days (Palmer et al., 2013). However, correlations between ΔOA and ΔCO throughout these flights were exceptionally weak, yielding R^2 values consistently well below 0.1, contrasting with values in the range 0.39–0.74 for flights B621-B624 and B626. These weak correlations from later flights suggest that sampled air masses lack a common emission source and instead represent extensive mixtures of different plumes following dispersion, or that emissions have been differentially processed to the extent that representative properties can no longer be distinguished. As a result, data from these flights were omitted from this analysis.

3 Results and discussion

3.1 Spatial and temporal variability in BB emissions properties

Measurements of OA in BB plumes during the BORTAS flights included within this analysis encompassed a wide range of ages, from directly at source to up to 5 days of aging. The extent of this diversity in age contributed to a high level of variability in plume properties, both across separate research flights and between individual plumes encountered in different periods of the same flight. Excess OA concentrations measured in-plume ranged from close to zero to around 180 $\mu g\,m^{-3}$, with maximum ΔCO concentrations approaching 1000 ppb. Vertical profiles of both species are shown in Fig. 1, revealing an overall increase in concentrations throughout the boundary layer to a peak at around 2000 m, before declining to background levels through the free troposphere. Significant elevations in both ΔOA and ΔCO occurred close to ground level, most likely as a result of influence from local sources. The observed decrease in concentration with altitude is more marked for ΔOA, which returns to background levels by 6000 m. Variability in ΔCO is much greater than ΔOA at higher altitudes. ΔCO concentrations of up to 800 ppb were observed between 5000–8000 m, whereas ΔOA did not exceed 30 $\mu g\,m^{-3}$. This disparity is attributed to the removal of OA from plumes encountered during flight B622 (20 July) by precipitation prior to sampling following

ACPD
14, 25095–25138, 2014

advection through clouds, as corroborated by meteorological observations and back trajectory models (Griffin et al., 2013; Taylor et al., 2013). Wet deposition of aerosol reduced ΔOA to background levels, while ΔCO concentrations remained elevated to similar levels as observed at lower altitudes. Despite their biomass burning origin, the absence of OA and BC from these plumes resulted in their omission from this analysis.

The change in combustion conditions between different periods of BORTAS is reflected in the contrast between loadings of particulate and gas-phase species. Concentrations in aged plumes sampled during flights B621–B624 consistently exceeded those at source from B626, irrespective of the effect of dilution as plumes dispersed into the ambient atmosphere. During flight B626, ΔOA peaked at around 50 $\mu g\,m^{-3}$, with concentrations in more aged plumes exceeding this level by a factor of four. ΔCO concentrations were also significantly elevated in aged plumes relative to fresh emissions. The contrast in properties between plumes of different ages is likely to be primarily affected by a change in the size and intensity of fires, rather than combustion phase alone, given the stronger association of OA production with predominantly smouldering combustion in the latter stages of fire evolution (Reid et al., 2005).

While the higher concentrations identified in aged plumes may be influenced to some extent by contributions from SOA, initial indications from calculated ΔOA/ΔCO ratios suggest this contribution did not provide any net increase in OA loadings. Normalising to a co-emitted, non-reactive tracer such as ΔCO provides an emission ratio (ER) when calculated at source, also denoted as a normalised excess mixing ratio (NEMR) for any other point in a plume away from source, and accounts for the effects of dispersion. These ratios can also be used as a marker for potential SOA formation, as the longer atmospheric lifetime of CO (~ 1 month) relative to that of OA (on the order of several weeks) makes it likely that any enhancement of the ratio between the two species will be a result of the addition of OA, rather than increased removal of CO in isolation. Figure 2 shows ΔOA/ΔCO for all 5 relevant BORTAS flights, with average values determined from the gradient of linear least squares regressions. Using this approach reveals that the average ΔOA/ΔCO close to source (0.190 ± 0.010, where

ACPD
14, 25095–25138, 2014

uncertainty represents the standard deviation in the fit) exceeds that for aged plumes (0.097 ± 0.002) by around 50 %, with an overall campaign average of 0.092 ± 0.002. Average ratios for individual flights sampling aged emissions range from 0.056 ± 0.003 (B624) to 0.114 ± 0.003 (B622), giving an overall range of 0.058. The level of average $\Delta OA/\Delta CO$ for fresh emissions from boreal forest fires during BORTAS falls between the upper extent derived from the eucalypt forests of northern Australia during ACTIVE (0.329), and lower ratios from several other campaigns where OA enhancements were comparatively reduced (0.019–0.065; Jolleys et al., 2012). Average $\Delta OA/\Delta CO$ from aged plumes during BORTAS was again within the range identified from previous field observations, although with closer proximity to ratios from the lower extent of the observed range, including aged boreal forest fire plumes sampled during the Arctic Research of the Composition of the Troposphere from Aircraft and Satellites (ARCTAS) campaign (Hecobian et al., 2011). The extent of variability amongst aged emissions during ACTIVE also exceeded that observed during BORTAS, with flights throughout the former campaign sampling plumes from fires in a number of different source regions. However, analysis of ERs from vegetation fires performed under laboratory conditions during the second Fire Lab At Missoula Experiment (FLAME II) also revealed extensive variability in $\Delta OA/\Delta CO$ directly at source, even amongst single plant species (Jolleys et al., 2014). The single source region from which BORTAS plumes originated could therefore still be expected to give rise to significantly contrasting $\Delta OA/\Delta CO$, while the effects of atmospheric processing during transportation provide further perturbation of initial ERs. Aged BORTAS plumes had been transported over extensive geographical and temporal scales, and provide an indication of the potential implications of OA losses during long-range transport. Average $\Delta OA/\Delta CO$ decreased progressively as the distance from source at which plumes were intercepted increased, with B622 performing a transit between Halifax and Quebec City, and B624 primarily sampling plumes over the North Atlantic off the eastern coast of Nova Scotia and Newfoundland.

ACPD
14, 25095–25138, 2014

3.2 Tracers for combustion conditions

While the evolution of ΔOA/ΔCO in aging plumes would appear to be strongly influenced by the effects of atmospheric processing, source conditions remain a critical factor in controlling OA production. Contrasts in ΔOA/ΔCO between fresh and aged OA are accompanied by varying properties with respect to the location and composition of plumes. Proportional contributions of OA mass fragment marker species differ between near and far-field measurements. f_{60} represents the prevalence of primary combustion products such as levoglucosan and is used as an indicator for fresh BB emissions (Schneider et al., 2006; Alfarra et al., 2007). Conversely, f_{44} is associated with the CO_2^+ ion derived from more aged OA as hydrocarbon fragments are oxidised to form organic acids (Zhang et al., 2005; Aiken et al., 2008), although m/z 44 has also been shown to be significantly elevated at source, dependent on combustion conditions (Weimer et al., 2008; Jolleys et al., 2014). While strongly associated with saturated hydrocarbon fragments, m/z 43 can also originate from oxidised compounds such as aldehydes and ketones (Alfarra et al., 2004). Large contributions of m/z 43 have been observed within the mass spectra of OA during the laboratory combustion of a range of biomass fuels, typically accounting for a greater proportion of total OA mass than any other detected fragments (Schneider et al., 2006). This dominance of m/z 43 above m/z 44 amongst even compounds with high oxygen contents suggests the former can be produced preferentially during the fragmentation of oxygenated molecules, and as such f_{43} may prove to be an appropriate indictor of OA oxygenation at source.

Variations in the average proportions of m/z 43, 44 and 60 in OA between fresh and aged plumes are widely observed throughout BORTAS, emphasising the contrasting properties of aerosol of different ages. Mean f_{44} for B626, which comprised the only measurements of fresh OA during BORTAS, was lower than all other flights at 0.086 ± 0.014, with mean values for B621-B624 ranging from 0.104 to 0.139. This trend between the near and far-field is consistent with observations of boreal forest fire plumes during ARCTAS, where f_{44} was shown to increase as a function of plume

ACPD
14, 25095–25138, 2014

transport time (Cubision et al., 2011; Hecobian et al., 2011). f_{60} was also shown to decrease concurrently with increasing f_{44} during ARCTAS, as a result of the oxidation of primary levoglucosan-type species with aging. However, mean f_{60} for BORTAS flight B626 was also amongst the lowest throughout the campaign at 0.007 ± 0.004. Averages were higher for B621-B623 (0.010–0.017), although B624 provided the lowest f_{60} with a mean of 0.005 ± 0.001.

While the higher mean f_{44} observed in the far-field is likely to primarily result from more extensive oxidation of OA after longer periods of aging, the transition to more smouldering-dominated combustion prior to sampling of near-field plumes could also have influenced observed changes in composition. Elevated levels of f_{60} in aged plumes are indicative of such an effect, as m/z 60 would be expected to constitute a greater proportion of fresh OA, given its typical progressive depletion through oxidation (Cubision et al., 2011). However, the relationships between f_{44}, f_{60} and combustion phase are known to be complex and subject to considerable uncertainty. Weimer et al. (2008) showed f_{60} to be more strongly associated with the initial flaming phase of combustion in wood burners used for domestic heating, while f_{44} was higher during the later stages of the burning process when smouldering combustion dominated. These trends are attributed to changes in combustion behaviour and the consumption of different fuel components at each stage of the fire. In contrast, Gao et al. (2003) reported significantly elevated levoglucosan concentrations from smouldering fires in southern Africa, and severe depletion in emissions from flaming fires. Furthermore, Lee et al. (2010) reported overall similarity in f_{60} across flaming and smouldering phases for open biomass fires carried out in a laboratory setting as part of FLAME II, while the ratio of levoglucosan to total organic carbon in filter samples from the same experiment shows a dependence on the fuel component burned (Sullivan et al., 2008). Although both f_{44} and f_{60} were more frequently at a maximum during flaming combustion in FLAME II burns (Jolleys et al., 2014), differences between phases were more pronounced for f_{44}, with less variation amongst f_{60}. This behaviour is expected to result from greater fire intensity during flaming combustion, although the specific effects

ACPD
14, 25095–25138, 2014

of increased intensity on OA composition through changing oxygen availability remain unclear.

Further indication of a shift in combustion phase is provided by the differences in f_{43} between fresh and aged plumes, for which respective mean values were 0.123 ± 0.013 and 0.088 ± 0.012. The low f_{44} and f_{60} for fresh OA suggest a dominance of smouldering fires, in agreement with the trends identified by Jolleys et al. (2014). Additional variations in plume properties appear to substantiate an association between f_{43} and smouldering combustion, including the correlation between periods of high f_{43} (> 0.1) and low $\Delta BC/\Delta OA$ (< 0.02) in both fresh and aged plumes, with production of BC expected to be at a maximum during flaming combustion (Reid and Hobbs, 1998). Absence of a prominent flaming phase close to source is also corroborated by very low BC mass loadings, and reduced $\Delta BC/\Delta OA$ relative to aged emissions, while the elevated $\Delta OA/\Delta CO$ from these fires is consistent with the enhanced OA production typical of smouldering combustion (Yokelson et al., 1997). The lower $\Delta OA/\Delta CO$ and f_{43}, but higher f_{44} and f_{60}, for aged OA would therefore be expected to derive from more intense, flaming-dominated combustion, which would also account for the significantly higher concentrations observed for ΔOA, ΔBC, ΔCO and ΔHCN despite plumes being progressively diluted over several days.

3.3 Effects of combustion conditions on vertical distributions

Altitudinal variations in plume composition further emphasise the importance of combustion conditions as a control on BB emissions and their propagation within the atmosphere. Profiles of aged plumes during BORTAS shown in Fig. 3 highlight the shift in properties between the upper and lower troposphere, with higher altitude plumes more typical of flaming combustion. The $\Delta BC/\Delta OA$ ratio is used as an indicator for the comparative contributions from flaming and smouldering combustion phases to the overall BB particulate loading (e.g. Grieshop et al., 2009), and is shown to increase through successive 500 m bins from 0.015 ± 0.003 at 500 m to 0.110 ± 0.055 at 6000 m, with the interquartile range increasing from 0.006 (2000 m) to 0.068 (5500 m). In contrast,

ACPD
14, 25095–25138, 2014

ΔOA/ΔCO decreases over the same range, revealing the stark contrasts in plume composition at different altitudes and the apparent influence of fire properties at source. Mean ΔOA/ΔCO stands at 0.155 ± 0.061 and 0.196 ± 0.103 for the two bins closest to the surface, declining to 0.038 ± 0.015 at 6000 m. The interquartile range also decreases from 0.147 to 0.044 between 1500 and 5500 m, reflecting an overall reduction in variability with altitude.

With the exception of a few isolated points, ΔBC/ΔOA only rises above 0.02 in higher plumes where f_{43} is below 0.09, and remains consistently low when f_{43} is above this level (Fig. 4). This trend is in part due to the greater production of BC under flaming conditions, as reflected by corresponding distributions of high BC mass concentration, f_{60} and CO_2 (Fig. 4a–c). Conversely, plumes sampled at lower altitudes exhibit characteristics more strongly associated with smouldering combustion (Fig. 4d), and are comparable to fresh plumes with regards to low levels of ΔBC/ΔOA and f_{60}, and high f_{43}. Weaker convection resulting from smouldering fires limits vertical transportation, retaining plumes within the boundary layer (Andreae et al., 1996; Warneke et al., 2006; Burling et al., 2011). The presence of flaming-derived emissions at higher altitudes alludes to an elevated injection height resulting from increased buoyancy and pyroconvection (Fromm et al., 2005; Damoah et al., 2006) driven by more intense fires earlier in the BORTAS campaign period (Fig. S2 in the Supplement). A similar dependence on combustion phase has previously been observed for the altitudinal distribution of different combustion products from boreal forest fires during ARCTAS (Kondo et al., 2011).

The altitudinal trends identified for ΔOA/ΔCO and ΔBC/ΔOA also show broad agreement with those of f_{43} and f_{60} respectively, with mean values for the former decreasing from 0.078 ± 0.003 to 0.128 ± 0.006 and latter increasing from 0.005 ± 0.001 to 0.015 ± 0.002. The directly opposing profiles of f_{43} and CO_2 (Fig. 3c and d), along with the correlation of increased f_{60} with CO_2 and BC mass at high altitudes (Fig. 5h and i), further underline the importance of initial combustion conditions for aged emissions. Minimum CO_2 concentrations within aged plumes were around 375 ppm, representing

ACPD
14, 25095–25138, 2014

a minimal elevation above typical background levels for boreal Canadian forest environments (Vay et al., 2011; Higuchi et al., 2003). Although the distribution of CO_2 clearly reflects the influence of the biosphere closer to the surface through uptake in photosynthesis, expected source profiles also appear to be largely conserved, further corroborated by the sustained correlation between periods of high f_{43} and low CO_2 and vice versa.

3.4 Aging as a driver for plume variability

Despite the apparent influence of combustion conditions on the vertical distribution and composition of aged emissions, the effects of transformations associated with atmospheric processing cannot be entirely discounted. Certain contrasting properties between emissions of different ages could also be less dependent on source conditions and more strongly influenced by processing throughout plume evolution. Differences between fresh and aged plumes in the respective relationships of total ΔOA loadings, and those normalised to ΔCO, with a number of tracers highlight the combined effects of source conditions and processing, and their changing influence with aging. Both ΔOA and ΔCO concentrations show a negative correlation with f_{44} (e.g. Fig. 5a and b) and positive correlation with f_{60} (e.g. Fig. 5f and g). These overriding trends remain consistent for emissions of all ages, although the nature of the relationship changes in each case. Linear relationships appear consistently for ΔOA ($R^2 = 0.51$ and 0.80 with f_{44} and f_{60} respectively) and ΔCO ($R^2 = 0.23$ and 0.49) in fresh emissions. The same relationships also persist to an extent for ΔOA/ΔCO in fresh plumes ($R^2 = 0.42$ and 0.47). However, at a greater distance from source, correlations for ΔOA and ΔCO are consistently below 0.3, while there is no relationship between ΔOA/ΔCO and either f_{44} or f_{60}. This disparity suggests that NEMRs in the far-field are less solely dependent on source conditions than ERs in the near-field, and are more strongly affected by further influences during aging.

In addition to providing a tracer for source profiles in aged BB emissions, ΔBC/ΔOA can also be used as an indicator for OA processing. Observations of increasing

ACPD
14, 25095–25138, 2014

ΔBC/ΔOA with aging have previously been attributed to the loss of OA mass through evaporation (Liousse et al., 1995). Similar behaviour has also been proposed as a possible cause of the overall reduction in ΔOA/ΔCO between BB plumes in the near and far-field throughout several campaigns across different global regions (Jolleys et al., 2012). Any decrease in ΔBC/ΔOA could therefore be considered a product, to a certain degree, of the addition of secondary organic mass from either the processing of BBOA or external sources. Measurements performed at lower altitudes (< 2000 m) during flights B621 and B622 provide possible evidence to support such an effect. Both BC mass and f_{60} remain low during these periods, at less than 0.5 μg m^{-3} and 0.01 respectively, consistent with wider observations of smouldering fire emissions at low altitude during BORTAS. However, ΔCO concentrations are also diminished and consistently below 100 ppb, relative to an average of 200 ppb for aged plumes, while ΔOA concentrations are comparable to levels in higher altitude, flaming-type plumes (∼ 20 μg m^{-3}). These trends, which diverge from the expected characteristics for emissions of this origin, are further compounded by high $\Delta O_3/\Delta CO$ (> 0.2), indicative of an elevated level of oxygenation and photochemical activity (Mason et al., 2001; Parrington et al., 2013). Formation of SOA from biogenic precursors has previously been observed in the forests of Ontario (Slowik et al., 2010). These SOA events were also characterised by ΔOA/ΔCO levels far in excess of those derived for BB emissions during the same study. In accordance with this trend, ΔOA/ΔCO within the low altitude plumes in B621 and B622 were consistently above the average for aged emissions (0.097), reaching as high as ∼ 0.4. There is subsequently considerable evidence to support biogenic SOA as a potential contributor to the OA burden during BORTAS, which could provide further enhancement of ΔOA/ΔCO as demonstrated by the Slowik et al. (2010) Ontario study. Whilst the further properties of aged plumes discussed here would suggest this effect is isolated and limited in its overall impact, it presents a further source of uncertainty for any attempts to develop parameterisations for the contribution of forest fires to regional and global OA budgets.

ACPD
14, 25095–25138, 2014

Although f_{60} displays a level of consistency with flaming combustion products in upper troposphere plumes, and increases on average with increasing altitude, further trends oppose the expected relationships for different combustion phases. Maximum concentrations of ΔOA, ΔBC, ΔCO and CO_2 all coincide with high f_{60} (0.025–0.300) and show a reduction as f_{60} decreases (Fig. 5f–i). Overall correlations between each species and f_{60} are all positive, albeit with varying fit coefficients. R^2 values were highest for CO_2 and ΔBC (0.52 and 0.47), reflecting their stronger associations with flaming combustion (Crutzen and Andreae, 1990; Reid et al., 2005). Correlations with ΔOA and ΔCO were weaker ($R^2 = 0.28$ and 0.23), as would be expected given production of each is greatest during the smouldering phase (Ferek et al., 1998; Andreae and Merlet, 2001; Gao et al., 2003). While trends with $\Delta O_3/\Delta CO$ show f_{60} to decrease with aging (Fig. 5j), the underlying relationships identified with all other species suggest f_{60} may prove to be a more resilient tracer for overall plume intensity rather than combustion conditions at long aging times. However, Petzold et al. (2007) demonstrated export efficiencies of up to 90 % for BC following intercontinental transport of boreal forest fire plumes. In the absence of significant removal through wet deposition, BC/ΔCO in plumes encountered at altitudes above 4 km remained consistent with typical source values, indicating that mixing of emissions can be suppressed where fire intensity is sufficient to generate elevated injection heights. Conversely, the weaker convection associated with smouldering combustion may lead to emissions being retained within the boundary layer, contributing to the observed enhancements in ΔOA/ΔCO and f_{43} at low altitudes.

3.5 Tracer evolution during BORTAS

The progression from f_{60} to f_{44} can provide a useful metric to assess the evolution of OA composition with aging. Figure 6 shows the nature of this progression for both fresh and aged OA, together with further trends with several additional parameters. A strong linear relationship ($R^2 = 0.72$) is identified for emissions close to source. However, these observations comprised measurements of three separate periods of flight B626, and

ACPD
14, 25095–25138, 2014

reveal a clear discrepancy for one of these periods. Measurements performed further to the east of the source region, on a transect from approximately 52.3° N, 90.0° W to 52.8° N, 91.3° W (a "downwind" plume) yielded higher f_{44} than any other fresh plumes, with f_{60} not exceeding 0.045. The two remaining sets of plumes ("source" plumes) were both encountered within a region where active fires were present at around 52.4–52.8° N, 93.0–93.7° W. Despite sampling taking place roughly two hours apart, and over a slightly different geographical extent, the f_{44}/f_{60} relationship remains highly consistent across all "source" plumes, with an R^2 of 0.82. The higher levels of f_{44} and absence of a trend with f_{60} in the "downwind" plume indicate OA is more heavily oxidised than in the fresher "source" plumes. This contrast in oxygenation is linked to other changes between plumes, including apparent photochemical age, which in this instance is represented by the $-\log(NO_x/NO_y)$ ratio (Kleinman et al., 2008; DeCarlo et al., 2008). Levels of the ratio are significantly elevated in the "downwind" plume from B626 (Fig. 6f, left panel), with an average of 1.45±0.43, exceeding the mean value of 1.09±0.29 for highly aged plumes sampled during flights B621-B624. CO_2 concentrations during this period are also higher than for the remainder of B626 (Fig. 6b, left panel), with an average of 378.6 ± 0.6 ppm compared to 375.0 ± 1.3 ppm closer to source. The $-\log(NO_x/NO_y)$ photochemical clock is also shown to increase throughout "source" plumes, with f_{44} and f_{60} changing in a manner consistent with the increasing oxidation of OA, and is further corroborated by a trend of increasing $\Delta O_3/\Delta CO$ (Fig. 6e, left panel). However, these changes also coincide with a trend of decreasing $\Delta OA/\Delta CO$ (Fig. 6c, left panel), belying the expected addition of OA mass resulting from increasing oxygenation. Average $\Delta OA/\Delta CO$ is similar for the two "source" plumes (0.165±0.042 and 0.180±0.045), but is lower in the more photochemically aged "downwind" plume (0.114 ± 0.015). It is difficult to speculate on the significance of any link between a higher rate of oxidation and an overall reduction in $\Delta OA/\Delta CO$ given the continuing uncertainty regarding the processes affecting OA in aging BB plumes. Yokelson et al. (2009) reported that $\Delta OA/\Delta CO$ increased by a factor of 2.3 over a period of 1.4 h for plumes from fires in the Yucatan region of Mexico, coinciding with a comparably high f_{44}/f_{60} gradient to

ACPD
14, 25095–25138, 2014

that in the "downwind" section of B626. Conversely, an increase in f_{44} has also been shown in conjunction with stable or even decreasing levels of $\Delta OA/\Delta CO$ (Capes et al., 2008; Cubison et al., 2011; Akagi et al., 2012; Jolleys et al., 2012), suggesting OA loss through evaporation has an equally important effect throughout plume evolution.

Linear relationships between f_{44} and f_{60} are weaker for more aged plumes sampled at a greater distance downwind, with an overall R^2 value for all plumes of 0.44 and individual flights ranging from 0.01 (B624) to 0.32 (B622). The overall decline of f_{60} again appears to be strongly influenced by distance from the source region and the physical age of plumes, decreasing from a maximum of ~ 0.027 in B622 to a minimum of ~ 0.004 in B624. An effect of dilution is evident, given the concurrent reduction in both ΔCO and CO_2 with decreasing f_{60} and increasing f_{44} (Fig. 6a and b, right panels). $\Delta O_3/\Delta CO$ shows the reverse progression, increasing with the oxygenation of OA (Fig. 6e, right panel), while $-\log(NO_x/NO_y)$ does not exhibit the strong trend observed for near-field measurements but is typically higher and reflects longer aging times (Fig. 6f). However, $-\log(NO_x/NO_y)$ ratios were highest on average for the "downwind" plume in B626, which did not provide any significant indication of net addition of OA mass. While the highest average $\Delta OA/\Delta CO$ ratio for an individual plume throughout the entirety of BORTAS was derived for one of the "source" plumes during B626, two aged plumes from B622 exhibited average $\Delta OA/\Delta CO$ of a similar magnitude (0.120 ± 0.080 and 0.119 ± 0.042), with each plume representing a different region of f_{44}/f_{60} space. Together with the overall lack of consistency between $\Delta OA/\Delta CO$ and f_{44}/f_{60} throughout aged plumes, and the subsequent contrast with plumes at source, this inconsistency further highlights the need for improved characterisation of the processes contributing towards aging of BBOA during long range transport.

The contrasting behaviours of various tracers throughout fresh and aged plumes highlights the different ways in which these properties can be used to evaluate influences on BBOA evolution. With regards to f_{44}, the consistently higher values observed in aged plumes, and the strong trends identified with indicators of photochemical aging such as $-\log(NO_x/NO_y)$ and $\Delta O_3/\Delta CO$ close to source (Fig. 6e and f, left panels),

ACPD
14, 25095–25138, 2014

substantiate its use as a tracer for OA aging. Although f_{60} exhibits the same clear relationship with $-\log(NO_x/NO_y)$ and $\Delta O_3/\Delta CO$ in fresh plumes, albeit reversed and decreasing with aging, values are higher on average amongst aged plumes. Given the overall trend of increasing f_{44} with decreasing f_{60} remains for aged OA, the longer periods of aging to which these plumes have been exposed would be expected to bring about a more extensive reduction in the latter tracer. The elevation in f_{60} relative to fresh plumes would therefore seem to stem from the contrasting dominant combustion phases associated with plumes of different ages, and the persistence of high levels in flaming-derived OA at greater altitudes. In contrast, f_{43} shows an overall reduction with aging, with mean values of 0.123±0.013 and 0.088±0.012 for near and far-field plumes respectively, consistent with the oxidation of primary OA components over time. However, overall trends with $-\log(NO_x/NO_y)$ and $\Delta O_3/\Delta CO$ in fresh plumes are generally positive, albeit with fairly weak correlation coefficients ($R^2 = 0.12$ and 0.34), resulting in f_{43} peaking at greater photochemical ages. This relationship contradicts that which would be expected in aging OA (Ng et al., 2010; Morgan et al., 2010), and suggests additional factors may be contributing to the observed variability in f_{43}. Values of f_{43} in fresh OA are almost entirely greater than 0.1, while this threshold is most frequently exceeded amongst aged OA in plumes below around 3000 m (Fig. 3d). These lower altitude plumes exhibit the same low $\Delta BC/\Delta OA$ levels as identified close to source (< 0.02), in contrast to the greater range in $\Delta BC/\Delta OA$ (up to 0.15) coinciding with lower f_{43} (Fig. 4). Differing distributions of f_{43} in aged plumes, and the prescribed similarities with near-field observations, may reflect an influence of changing combustion conditions, with f_{43} seemingly more prominent in OA from smouldering fires. As a result, f_{43} may prove to be a more suitable tracer for source conditions rather than the effects of aging, although comparison between different combustion phases at source would be required in order to fully constrain any such relationship.

ACPD
14, 25095–25138, 2014

3.6 Campaign intercomparison and evaluation of f_{44} and f_{60} tracers

The progression of f_{44} and f_{60} throughout BORTAS shows a number of similarities with observations from other field campaigns and laboratory experiments. Distributions for fresh and aged emissions from BORTAS and montane forest fires during the Megacities Initiative: local and Global Research Observations (MILAGRO) campaign are presented in Fig. 7, along with data from numerous plumes measured during ARCTAS-B. Data are also shown for the combustion of boreal forest plant species under laboratory conditions as part of FLAME II. Similar trends in f_{44}/f_{60} for fresh and aged emissions are identified for BORTAS and MILAGRO, with average f_{44} increasing with aging in both cases. A significant contrast is also evident in the distributions of f_{60}, which is higher on average for fresh plumes in MILAGRO and aged plumes in BORTAS, possibly as a result of the reduced intensity of fires sampled close to source. Average $\Delta OA/\Delta CO$ is again lower for the aged fraction in MILAGRO, decreasing from 0.051 ± 0.001 in fresh plumes to 0.041 ± 0.001 (Jolleys et al., 2012), consistent with a loss of OA. The lower magnitude of these ratios is likely to be a consequence of different fuel properties and resulting combustion conditions, as strongly-flaming grass fires are expected to have made a significant contribution to smoke plumes sampled at the Paso de Cortes measurement site (Jolleys et al., 2013). Figure 7 also emphasises the differences in emissions from boreal forest fires during ARCTAS-B and BORTAS. Plumes encountered close to source in each campaign exhibit contrasting levels of f_{60}, reflecting the dominance of different combustion phases in each set of measurements. Unlike the heavily smouldering fires sampled in flight B626, the plume from a fire at Lake McKay in northwestern Saskatchewan was produced by highly intense, flaming fires (Cubison et al., 2011). The Lake McKay fires subsequently yielded higher f_{60} than was observed for any BORTAS plumes, peaking at around 0.05. As the Lake McKay plume was tracked downwind, f_{44} increased to ~ 0.12, comparable to the upper extent for fresh plumes in BORTAS. Although f_{60} decreased to ~ 0.015, this level remained above the majority of the distribution from BORTAS. Similarly high levels of f_{60} were observed for black

ACPD
14, 25095–25138, 2014

spruce fires during FLAME II. However, f_{44} from these burns was generally exceptionally low, as would be expected given the direct measurement at source and lack of aging. Higher f_{44} comparable to the range identified in ambient emissions did occur in chamber fires for plant species representing environments other than boreal forests, with average values particularly high for chaparral fuels. Montane forest fuels, which like the boreal equivalent comprised samples of coniferous species, also yielded f_{44} up to ~ 0.15, although such fires largely involved drier, woody plant material leading to more flaming-dominated combustion (Jolleys et al., 2014).

The different f_{44} and f_{60} regimes in ambient and chamber fires, and their conflicting relationships with combustion phases, suggest their use as tracers for processing of BBOA is highly dependent on both fire properties and experimental conditions. Throughout FLAME II, f_{44} was shown to be more strongly associated with flaming combustion, as increased intensity and turbulent mixing enhanced the supply of oxygen to fires. In contrast, the rapid increase in f_{44} in fresh OA from smouldering fires during BORTAS, to levels comparable to more extensively aged plumes, indicate that f_{44} is strongly influenced by post-emission processing under ambient conditions. Relationships with f_{60} are more consistent, being higher on average more frequently for flaming-dominated fires under laboratory conditions, and showing a stronger association with seemingly flaming-derived aged emissions during BORTAS. Probability density functions (PDFs) for f_{44} and f_{60} in fresh and aged emissions from BORTAS, along with source emissions from fires involving boreal and montane forest fuels during FLAME II, are shown in Fig. 8. The clear separation in f_{44} distributions between chamber and ambient measurements reflects the role of aging in determining the level of oxidation in BBOA, as further evidenced by the enhancement in plumes in the far-field above those at source. However, the trend of increasing f_{44} in fresh plumes suggests that this processing can occur over very short timescales under certain atmospheric conditions. Rapid oxidation of BB smoke plumes has previously been inferred from the addition of secondary OA mass within ~ 1 h of emission (Gao et al., 2003; Yokelson et al., 2009), corroborating the BORTAS trend. Values of f_{44} coinciding with peak concentrations for

ACPD
14, 25095–25138, 2014

a number of combustion products are also shown in Fig. 8. These peak concentrations show a good agreement with prescribed combustion phase relationships for FLAME II data, with ΔCO_2 reaching a maximum when f_{44} is higher, and hence combustion more flaming-dominated, while ΔOA and ΔCO peak at a lower f_{44}. The same trends are also observed throughout BORTAS, with peak concentrations for ΔCO_2 and ΔBC coinciding with higher levels of f_{44} than those of ΔCO or ΔOA. PDFs for f_{60} exhibit the same trend amongst ambient plumes, shifting to higher values with aging. Distributions are also broadened for emissions from chamber burns, for which levoglucosan-type species constitute a larger proportion of the total OA mass. The very low peak for near-field BORTAS plumes could be influenced by both the absence of a significant flaming phase and subsequent oxidation of primary OA (Cubison et al., 2011), contributing to the increase in f_{44}. The variable gradients for f_{44}/f_{60} regressions (Fig. 7) indicate a slower rate of decay for levoglucosan-type OA in aged BORTAS plumes compared to their equivalents from MILAGRO. Furthermore, mean f_{60} in aged MILAGRO plumes (0.006 ± 0.003) was lower than in fresh plumes (0.018 ± 0.006), while the opposite was true for BORTAS plumes (0.012 ± 0.005 and 0.007 ± 0.004 respectively). As such, the slower decline of f_{60} and potential influences from more strongly flaming combustion may contribute towards the observed enhancement in aged BORTAS plumes, while a faster rate of oxidation and largely smouldering fires reduce levels closer to source.

4 Conclusions

Smoke plumes from Canadian boreal forest fires have been shown to exhibit highly variable properties over a range of ages. Average ΔOA/ΔCO in plumes sampled close to source (0.190 ± 0.010) exceed ratios in the far-field (0.056 ± 0.003 to 0.114 ± 0.003), reaffirming an absence of significant net SOA formation for aging BB emissions, at least to an extent that provides an elevation above initial OA production at source. An absence of increasing ΔOA/ΔCO has been widely observed in previous BB assessments, with a similar trend in BORTAS further emphasising the importance of source

ACPD
14, 25095–25138, 2014

conditions. High levels of typical flaming combustion products were identified in highly aged plumes following transportation over a period of several days. Enhancements in $\Delta BC/\Delta OA$ and f_{60} were most prominent within the free troposphere, typically displaying an overall increase with altitude, while aged OA sampled within the boundary layer showed stronger evidence for production by smouldering combustion. Plume injection height, as determined by combustion conditions at source, may therefore have a pivotal influence on the long-range retention of initial plume properties.

Aging of BBOA during BORTAS has been extensively evaluated using the key tracers f_{44} and f_{60} from the AMS mass spectrum. An enhancement in f_{44} was determined for far-field plumes, where the mean value of 0.121 ± 0.016 significantly exceeded that in the near-field (0.086 ± 0.014). Similarly, f_{60} remained higher in aged plumes (0.012 ± 0.005) than those close to source (0.007 ± 0.004), in spite of the concurrent increase in oxygenation and expected processing of primary OA components. These trends highlight the importance of both source conditions and processing for OA composition in BB plumes. While the influence of combustion phase on f_{44} remains highly uncertain given contrasting relationships with smouldering and flaming combustion reported in different studies, increases observed close to source suggest oxidation can occur over very short timescales after emission. This rapid processing is further corroborated by concurrent increases in photochemical tracers such as $\Delta O_3/\Delta CO$ and $-\log(NO_x/NO_y)$ ratios in plumes sampled at source. The increasing oxygenation of BBOA is not accompanied by an increase in $\Delta OA/\Delta CO$, which shows no significant change with $\Delta O_3/\Delta CO$ and decreases on average with $-\log(NO_x/NO_y)$. A lack of $\Delta OA/\Delta CO$ enhancement irrespective of evidence for wider transformations therefore further substantiates the impact of OA losses in aging BB plumes.

Presenting the changing composition of BBOA in f_{44}/f_{60} space reveals a consistent progression from high f_{60} to high f_{44} as primary levoglucosan-like species are lost through oxidation. Similar transitions occur across multiple datasets encompassing smoke plumes of varying origins and ages, although the gradients and extents of distributions show some variability between campaigns. Levels of f_{44} are also comparatively

ACPD
14, 25095–25138, 2014

depleted in chamber burns of boreal forest fuels. The absence of aging and a strong association with flaming combustion, and hence oxygen supply through entrainment, in these experiments denote alternative tracer functions under laboratory and ambient conditions. While f_{44} can act as an indicator for oxygenation through combustion processes in chamber experiments, the influence of aging is likely to limit such application for ambient emissions. However, f_{60} has been shown to act as a long-lived tracer for BB emissions, despite evidence for an overall reduction with increasing f_{44}.

Analysis of measurements performed during the BORTAS campaign has provided further insight to the variability associated with BB emissions and the processes affecting changes in BBOA loadings and composition over time. However, there remains considerable uncertainty regarding the main drivers of OA processing. While data from BORTAS provide evidence for the influence of a range of source and aging processes, the extents of any effects on aging BBOA are unclear, particularly with regard to their consistency across different environments and fire types. Key trends identified in this analysis, such as the comparatively lower levels of f_{60} close to source, contradict previous findings and highlight the lack of consistency prevalent amongst many aspects of investigations focusing on BB emissions. Further research specifically targeting these areas of uncertainty is therefore essential in order to understand the cause of these disparities and provide more reliable parameterisations of BB contributions to the atmospheric aerosol burden.

The Supplement related to this article is available online at doi:10.5194/acpd-14-25095-2014-supplement.

Acknowledgements. The authors would like to acknowledge financial support from the United Kingdom Natural Environment Research Council (NERC) under grant number NE/F017391/1, and thank all those involved in the BORTAS project. Airborne data was obtained using the FAAM BAe-146 Atmospheric Research Aircraft (ARA) operated by Directflight Ltd (DFL) and managed by the Facility for Airborne Atmospheric Measurements (FAAM), which is a joint entity

ACPD
14, 25095–25138, 2014

of NERC and the UK Meteorological Office. M. D. Jolleys was supported by a NERC studentship NE/H525162/1. P. I. Palmer also acknowledges support from the Leverhulme Trust.

References

Aiken, A. C., DeCarlo, P. F., Kroll, J. H., Worsnop, D. R., Huffman, J. A., Docherty, K. S., Ulbrich, I. M., Mohr, C., Kimmel, J. R., Sueper, D., Sun, Y., Zhang, Q., Trimborn, A., Northway, M., Ziemann, P. J., Canagaratna, M. R., Onasch, T. B., Alfarra, M. R., Prevot, A. S. H., Dommen, J., Duplissy, J., Metzger, A., Baltensperger, U., and Jimenez, J. L.: O/C and OM/OC ratios of primary, secondary, and ambient organic aerosols with high-resolution time-of-flight aerosol mass spectrometry, Environ. Sci. Technol., 42, 4478–4485, doi:10.1021/es703009q, 2008.

Aiken, A. C., Salcedo, D., Cubison, M. J., Huffman, J. A., DeCarlo, P. F., Ulbrich, I. M., Docherty, K. S., Sueper, D., Kimmel, J. R., Worsnop, D. R., Trimborn, A., Northway, M., Stone, E. A., Schauer, J. J., Volkamer, R. M., Fortner, E., de Foy, B., Wang, J., Laskin, A., Shutthanandan, V., Zheng, J., Zhang, R., Gaffney, J., Marley, N. A., Paredes-Miranda, G., Arnott, W. P., Molina, L. T., Sosa, G., and Jimenez, J. L.: Mexico City aerosol analysis during MILAGRO using high resolution aerosol mass spectrometry at the urban supersite (T0) – Part 1: Fine particle composition and organic source apportionment, Atmos. Chem. Phys., 9, 6633–6653, doi:10.5194/acp-9-6633-2009, 2009.

Akagi, S. K., Yokelson, R. J., Wiedinmyer, C., Alvarado, M. J., Reid, J. S., Karl, T., Crounse, J. D., and Wennberg, P. O.: Emission factors for open and domestic biomass burning for use in atmospheric models, Atmos. Chem. Phys., 11, 4039–4072, doi:10.5194/acp-11-4039-2011, 2011.

Akagi, S. K., Craven, J. S., Taylor, J. W., McMeeking, G. R., Yokelson, R. J., Burling, I. R., Urbanski, S. P., Wold, C. E., Seinfeld, J. H., Coe, H., Alvarado, M. J., and Weise, D. R.: Evolution of trace gases and particles emitted by a chaparral fire in California, Atmos. Chem. Phys., 12, 1397–1421, doi:10.5194/acp-12-1397-2012, 2012.

Alfarra, M. R., Coe, H., Allan, J. D., Bower, K. N., Boudries, H., Canagaratna, M. R., Jimenez, J. L., Jayne, J. T., Garforth, A. A., Li, S. M., and Worsnop, D. R.: Characterization of urban and rural organic particulate in the Lower Fraser Valley using two Aerodyne Aerosol Mass Spectrometers, Atmos. Environ., 38, 5745–5758, doi:10.1016/j.atmosenv.2004.01.054, 2004.

ACPD
14, 25095–25138, 2014

Alfarra, M. R., Prevot, A. S. H., Szidat, S., Sandradewi, J., Weimer, S., Lanz, V. A., Schreiber, D., Mohr, M., and Baltensperger, U.: Identification of the mass spectral signature of organic aerosols from wood burning emissions, Environ. Sci. Technol., 41, 5770–5777, doi:10.1021/es062289b, 2007.

Andreae, M. O. and Merlet, P.: Emission of trace gases and aerosols from biomass burning, Global Biogeochem. Cy., 15, 955–966, 2001.

Andreae, M. O., Atlas, E., Cachier, H., Cofer III, W. R., Harris, G. W., Helas, G., Koppmann, R., Lacaux, J.-P., and Ward, D. E.: Trace gas and aerosol emissions from savanna fires, in: Biomass Burning and Global Change, edited by: Levine, S., MIT Press, Cambridge, Mass., 278–295, 1996.

Bahreini, R., Jimenez, J. L., Wang, J., Flagan, R. C., Seinfeld, J. H., Jayne, J. T., and Worsnop, D. R.: Aircraft-based aerosol size and composition measurements during ACE-Asia using an Aerodyne aerosol mass spectrometer, J. Geophys. Res.-Atmos., 108, 8645, doi:10.1029/2002jd003226, 2003.

Bond, T. C., Streets, D. G., Yarber, K. F., Nelson, S. M., Woo, J. H., and Klimont, Z.: A technology-based global inventory of black and organic carbon emissions from combustion, J. Geophys. Res.-Atmos., 109, D14203, doi:10.1029/2003jd003697, 2004.

Burling, I. R., Yokelson, R. J., Akagi, S. K., Urbanski, S. P., Wold, C. E., Griffith, D. W. T., Johnson, T. J., Reardon, J., and Weise, D. R.: Airborne and ground-based measurements of the trace gases and particles emitted by prescribed fires in the United States, Atmos. Chem. Phys., 11, 12197–12216, doi:10.5194/acp-11-12197-2011, 2011.

Canagaratna, M. R., Jayne, J. T., Jimenez, J. L., Allan, J. D., Alfarra, M. R., Zhang, Q., Onasch, T. B., Drewnick, F., Coe, H., Middlebrook, A., Delia, A., Williams, L. R., Trimborn, A. M., Northway, M. J., DeCarlo, P. F., Kolb, C. E., Davidovits, P., and Worsnop, D. R.: Chemical and microphysical characterization of ambient aerosols with the aerodyne aerosol mass spectrometer, Mass Spectrom. Rev., 26, 185–222, doi:10.1002/mas.20115, 2007.

Capes, G., Johnson, B., McFiggans, G., Williams, P. I., Haywood, J., and Coe, H.: Aging of biomass burning aerosols over West Africa: aircraft measurements of chemical composition, microphysical properties, and emission ratios, J. Geophys. Res.-Atmos., 113, D00C15, doi:10.1029/2008jd009845, 2008.

Crosier, J., Allan, J. D., Coe, H., Bower, K. N., Formenti, P., and Williams, P. I.: Chemical composition of summertime aerosol in the Po Valley (Italy), northern Adriatic and Black Sea, Q. J. Roy. Meteor. Soc., 133, 61–75, doi:10.1002/qj.88, 2007.

ACPD
14, 25095–25138, 2014

Crounse, J. D., DeCarlo, P. F., Blake, D. R., Emmons, L. K., Campos, T. L., Apel, E. C., Clarke, A. D., Weinheimer, A. J., McCabe, D. C., Yokelson, R. J., Jimenez, J. L., and Wennberg, P. O.: Biomass burning and urban air pollution over the Central Mexican Plateau, Atmos. Chem. Phys., 9, 4929–4944, doi:10.5194/acp-9-4929-2009, 2009.

Crutzen, P. J. and Andreae, M. O.: Biomass burning in the tropics – impact on atmospheric chemistry and biogeochemical cycles, Science, 250, 1669–1678, doi:10.1126/science.250.4988.1669, 1990.

Cubison, M. J., Ortega, A. M., Hayes, P. L., Farmer, D. K., Day, D., Lechner, M. J., Brune, W. H., Apel, E., Diskin, G. S., Fisher, J. A., Fuelberg, H. E., Hecobian, A., Knapp, D. J., Mikoviny, T., Riemer, D., Sachse, G. W., Sessions, W., Weber, R. J., Weinheimer, A. J., Wisthaler, A., and Jimenez, J. L.: Effects of aging on organic aerosol from open biomass burning smoke in aircraft and laboratory studies, Atmos. Chem. Phys., 11, 12049–12064, doi:10.5194/acp-11-12049-2011, 2011.

Damoah, R., Spichtinger, N., Servranckx, R., Fromm, M., Eloranta, E. W., Razenkov, I. A., James, P., Shulski, M., Forster, C., and Stohl, A.: A case study of pyro-convection using transport model and remote sensing data, Atmos. Chem. Phys., 6, 173–185, doi:10.5194/acp-6-173-2006, 2006.

DeCarlo, P. F., Dunlea, E. J., Kimmel, J. R., Aiken, A. C., Sueper, D., Crounse, J., Wennberg, P. O., Emmons, L., Shinozuka, Y., Clarke, A., Zhou, J., Tomlinson, J., Collins, D. R., Knapp, D., Weinheimer, A. J., Montzka, D. D., Campos, T., and Jimenez, J. L.: Fast airborne aerosol size and chemistry measurements above Mexico City and Central Mexico during the MILAGRO campaign, Atmos. Chem. Phys., 8, 4027–4048, doi:10.5194/acp-8-4027-2008, 2008.

Di Carlo, P., Aruffo, E., Busilacchio, M., Giammaria, F., Dari-Salisburgo, C., Biancofiore, F., Visconti, G., Lee, J., Moller, S., Reeves, C. E., Bauguitte, S., Forster, G., Jones, R. L., and Ouyang, B.: Aircraft based four-channel thermal dissociation laser induced fluorescence instrument for simultaneous measurements of NO_2, total peroxy nitrate, total alkyl nitrate, and HNO_3, Atmos. Meas. Tech., 6, 971–980, doi:10.5194/amt-6-971-2013, 2013.

Drewnick, F., Hings, S. S., DeCarlo, P. F., Jayne, J. T., Gonin, M., Fuhrer, K., Weimer, S., Jimenez, J. L., Demerjian, K. L., Borrmann, S., and Worsnop, D. R.: A new time-of-flight aerosol mass spectrometer (TOF-AMS) – instrument description and first field deployment, Aerosol Sci. Tech., 39, 637–658, doi:10.1080/02786820500182040, 2005.

ACPD
14, 25095–25138, 2014

Ferek, R. J., Reid, J. S., Hobbs, P. V., Blake, D. R., and Liousse, C.: Emission factors of hydrocarbons, halocarbons, trace gases and particles from biomass burning in Brazil, J. Geophys. Res.-Atmos., 103, 32107–32118, 1998.

Forster, P., Artaxo, P., Berntse, T., Betts, R., Fahey, D. W., Haywood, J., Lean, J., Lowe, D. C., Myhre, G., Nganga, J., Prinn, R., Raga, G., Schulz, M., Van Dorland, R., Bodeker, G., Boucher, O., Collins, W. D., Conway, T. J., Dlugokencky, E., Elkins, J. W., Etheridge, D., Foukal, P., Fraser, P., Geller, M., Joos, F., Keeling, C. D., Keeling, R., Kinne, S., Lassey, K., Lohmann, U., Manning, A. C., Montzka, S., Oram, D., O'Shaughnessy, K., Piper, S., Plattner, G.-K., Ponater, M., Ramankutty, N., Reid, G., Rind, D., Rosenlof, K., Sausen, R., Schwarzkopf, D., Solanki, S. K., Stenchikov, G., Stuber, N., Takemura, T., Textor, C., Wang, R., Weiss, R., and Whorf, T.: Changes in atmospheric constituents and in radiative forcing, in: Climate Change 2007: The Physical Science Basis, Contribution of Working Group I to the Fourth Assessment Report of the Intergovernmental Panel on Climate Change, edited by: Solomon, S. D., Qin, M., Manning, Z., Chen, M., Marquis, K. B., Averyt, M. T., and Miller, H. L., Cambridge University Press, Cambridge, UK and New York, NY, USA, 129–234, 2007.

Fromm, M., Bevilacqua, R., Servranckx, R., Rosen, J., Thayer, J. P., Herman, J., and Larko, D.: Pyro-cumulonimbus injection of smoke to the stratosphere: observations and impact of a super blowup in northwestern Canada on 3–4 August 1998, J. Geophys. Res.-Atmos., 110, D08205, doi:10.1029/2004jd005350, 2005.

Gao, S., Hegg, D. A., Hobbs, P. V., Kirchstetter, T. W., Magi, B. I., and Sadilek, M.: Water-soluble organic components in aerosols associated with savanna fires in southern Africa: identification, evolution, and distribution, J. Geophys. Res.-Atmos., 108, 8491, doi:10.1029/2002jd002324, 2003.

Grieshop, A. P., Logue, J. M., Donahue, N. M., and Robinson, A. L.: Laboratory investigation of photochemical oxidation of organic aerosol from wood fires 1: measurement and simulation of organic aerosol evolution, Atmos. Chem. Phys., 9, 1263–1277, doi:10.5194/acp-9-1263-2009, 2009.

Griffin, D., Walker, K. A., Franklin, J. E., Parrington, M., Whaley, C., Hopper, J., Drummond, J. R., Palmer, P. I., Strong, K., Duck, T. J., Abboud, I., Bernath, P. F., Clerbaux, C., Coheur, P.-F., Curry, K. R., Dan, L., Hyer, E., Kliever, J., Lesins, G., Maurice, M., Saha, A., Tereszchuk, K., and Weaver, D.: Investigation of CO, C_2H_6 and aerosols in a boreal fire plume over eastern Canada during BORTAS 2011 using ground- and satellite-based observations

ACPD
14, 25095–25138, 2014

and model simulations, Atmos. Chem. Phys., 13, 10227–10241, doi:10.5194/acp-13-10227-2013, 2013.

Hallquist, M., Wenger, J. C., Baltensperger, U., Rudich, Y., Simpson, D., Claeys, M., Dommen, J., Donahue, N. M., George, C., Goldstein, A. H., Hamilton, J. F., Herrmann, H., Hoffmann, T., Iinuma, Y., Jang, M., Jenkin, M. E., Jimenez, J. L., Kiendler-Scharr, A., Maenhaut, W., McFiggans, G., Mentel, Th. F., Monod, A., Prévôt, A. S. H., Seinfeld, J. H., Surratt, J. D., Szmigielski, R., and Wildt, J.: The formation, properties and impact of secondary organic aerosol: current and emerging issues, Atmos. Chem. Phys., 9, 5155–5236, doi:10.5194/acp-9-5155-2009, 2009.

Hecobian, A., Liu, Z., Hennigan, C. J., Huey, L. G., Jimenez, J. L., Cubison, M. J., Vay, S., Diskin, G. S., Sachse, G. W., Wisthaler, A., Mikoviny, T., Weinheimer, A. J., Liao, J., Knapp, D. J., Wennberg, P. O., Kürten, A., Crounse, J. D., Clair, J. St., Wang, Y., and Weber, R. J.: Comparison of chemical characteristics of 495 biomass burning plumes intercepted by the NASA DC-8 aircraft during the ARCTAS/CARB-2008 field campaign, Atmos. Chem. Phys., 11, 13325–13337, doi:10.5194/acp-11-13325-2011, 2011.

Hennigan, C. J., Miracolo, M. A., Engelhart, G. J., May, A. A., Presto, A. A., Lee, T., Sullivan, A. P., McMeeking, G. R., Coe, H., Wold, C. E., Hao, W.-M., Gilman, J. B., Kuster, W. C., de Gouw, J., Schichtel, B. A., Collett Jr., J. L., Kreidenweis, S. M., and Robinson, A. L.: Chemical and physical transformations of organic aerosol from the photo-oxidation of open biomass burning emissions in an environmental chamber, Atmos. Chem. Phys., 11, 7669–7686, doi:10.5194/acp-11-7669-2011, 2011.

Heringa, M. F., DeCarlo, P. F., Chirico, R., Tritscher, T., Dommen, J., Weingartner, E., Richter, R., Wehrle, G., Prévôt, A. S. H., and Baltensperger, U.: Investigations of primary and secondary particulate matter of different wood combustion appliances with a high-resolution time-of-flight aerosol mass spectrometer, Atmos. Chem. Phys., 11, 5945–5957, doi:10.5194/acp-11-5945-2011, 2011.

Higuchi, K., Worthy, D., Chan, D., and Shashkov, A.: Regional source/sink impact on the diurnal, seasonal and inter-annual variations in atmospheric CO_2 at a boreal forest site in Canada, Tellus B, 55, 115–125, doi:10.1034/j.1600-0889.2003.00062.x, 2003.

Iinuma, Y., Bruggemann, E., Gnauk, T., Muller, K., Andreae, M. O., Helas, G., Parmar, R., and Herrmann, H.: Source characterization of biomass burning particles: the combustion of selected European conifers, African hardwood, savanna grass, and German and Indonesian peat, J. Geophys. Res.-Atmos., 112, D08209, doi:10.1029/2006jd007120, 2007.

ACPD
14, 25095–25138, 2014

J. L., Jimenez, Canagaratna, M. R., Donahue, N. M., Prevot, A. S. H., Zhang, Q., Kroll, J. H., DeCarlo, P. F., Allan, J. D., Coe, H., Ng, N. L., Aiken, A. C., Docherty, K. S., Ulbrich, I. M., Grieshop, A. P., Robinson, A. L., Duplissy, J., Smith, J. D., Wilson, K. R., Lanz, V. A., Hueglin, C., Sun, Y. L., Tian, J., Laaksonen, A., Raatikainen, T., Rautiainen, J., Vaattovaara, P., Ehn, M., Kulmala, M., Tomlinson, J. M., Collins, D. R., Cubison, M. J., Dunlea, E. J., Huffman, J. A., Onasch, T. B., Alfarra, M. R., Williams, P. I., Bower, K., Kondo, Y., Schneider, J., Drewnick, F., Borrmann, S., Weimer, S., Demerjian, K., Salcedo, D., Cottrell, L., Griffin, R., Takami, A., Miyoshi, T., Hatakeyama, S., Shimono, A., Sun, J. Y., Zhang, Y. M., Dzepina, K., Kimmel, J. R., Sueper, D., Jayne, J. T., Herndon, S. C., Trimborn, A. M., Williams, L. R., Wood, E. C., Middlebrook, A. M., Kolb, C. E., Baltensperger, U., and Worsnop, D. R.: Evolution of organic aerosols in the atmosphere, Science, 326, 1525–1529, doi:10.1126/science.1180353, 2009.

Jolleys, M. D., Coe, H., McFiggans, G., Capes, G., Allan, J. D., Crosier, J., Williams, P. I., Allen, G., Bower, K. N., Jimenez, J. L., Russell, L. M., Grutter, M., and Baumgardner, D.: Characterizing the aging of biomass burning organic aerosol by use of mixing ratios: a meta-analysis of four regions, Environ. Sci. Technol., 46, 13093–13102, doi:10.1021/es302386v, 2012.

Jolleys, M. D., Coe, H., McFiggans, G., McMeeking, G. R., Lee, T., Kreidenweis, S. M., Collett Jr., J. L., and Sullivan, A. P.: Organic Aerosol Emission Ratios from the Laboratory Combustion of Biomass Fuels, J. Geophys. Res.-Atmos., in review, 2014.

Kleinman, L. I., Springston, S. R., Daum, P. H., Lee, Y.-N., Nunnermacker, L. J., Senum, G. I., Wang, J., Weinstein-Lloyd, J., Alexander, M. L., Hubbe, J., Ortega, J., Canagaratna, M. R., and Jayne, J.: The time evolution of aerosol composition over the Mexico City plateau, Atmos. Chem. Phys., 8, 1559–1575, doi:10.5194/acp-8-1559-2008, 2008.

Kondo, Y., Matsui, H., Moteki, N., Sahu, L., Takegawa, N., Kajino, M., Zhao, Y., Cubison, M. J., Jimenez, J. L., Vay, S., Diskin, G. S., Anderson, B., Wisthaler, A., Mikoviny, T., Fuelberg, H. E., Blake, D. R., Huey, G., Weinheimer, A. J., Knapp, D. J., and Brune, W. H.: Emissions of black carbon, organic, and inorganic aerosols from biomass burning in North America and Asia in 2008, J. Geophys. Res.-Atmos., 116, D08204, doi:10.1029/2010jd015152, 2011.

Le Breton, M., McGillen, M. R., Muller, J. B. A., Bacak, A., Shallcross, D. E., Xiao, P., Huey, L. G., Tanner, D., Coe, H., and Percival, C. J.: Airborne observations of formic acid using a chemical ionization mass spectrometer, Atmos. Meas. Tech., 5, 3029–3039, doi:10.5194/amt-5-3029-2012, 2012.

ACPD
14, 25095–25138, 2014

Le Breton, M., Bacak, A., Muller, J. B. A., O'Shea, S. J., Xiao, P., Ashfold, M. N. R., Cooke, M. C., Batt, R., Shallcross, D. E., Oram, D. E., Forster, G., Bauguitte, S. J.-B., Palmer, P. I., Parrington, M., Lewis, A. C., Lee, J. D., and Percival, C. J.: Airborne hydrogen cyanide measurements using a chemical ionisation mass spectrometer for the plume identification of biomass burning forest fires, Atmos. Chem. Phys., 13, 9217–9232, doi:10.5194/acp-13-9217-2013, 2013.

Lee, T., Sullivan, A. P., Mack, L., Jimenez, J. L., Kreidenweis, S. M., Onasch, T. B., Worsnop, D. R., Malm, W., Wold, C. E., Hao, W. M., and Collett Jr., J. L.: Chemical smoke marker emissions during flaming and smoldering phases of laboratory open burning of wildland fuels, Aerosol Sci. Tech., 44, i–v, doi:10.1080/02786826.2010.499884, 2010.

Li, Q. B., Jacob, D. J., Bey, I., Yantosca, R. M., Zhao, Y. J., Kondo, Y., and Notholt, J.: Atmospheric hydrogen cyanide (HCN): biomass burning source, ocean sink?, Geophys. Res. Lett., 27, 357–360, doi:10.1029/1999gl010935, 2000.

Liousse, C., Devaux, C., Dulac, F., and Cachier, H.: Aging of savanna biomass burning aerosols – consequences on their optical properties, J. Atmos. Chem., 22, 1–17, doi:10.1007/bf00708178, 1995.

Mason, S. A., Field, R. J., Yokelson, R. J., Kochivar, M. A., Tinsley, M. R., Ward, D. E., and Hao, W. M.: Complex effects arising in smoke plume simulations due to inclusion of direct emissions of oxygenated organic species from biomass combustion, J. Geophys. Res.-Atmos., 106, 12527–12539, 2001.

McMeeking, G. R., Kreidenweis, S. M., Baker, S., Carrico, C. M., Chow, J. C., Collett Jr., J. L., Hao, W. M., Holden, A. S., Kirchstetter, T. W., Malm, W. C., Moosmueller, H., Sullivan, A. P., and Wold, C. E.: Emissions of trace gases and aerosols during the open combustion of biomass in the laboratory, J. Geophys. Res.-Atmos., 114, D19210, doi:10.1029/2009jd011836, 2009.

Morgan, W. T., Allan, J. D., Bower, K. N., Capes, G., Crosier, J., Williams, P. I., and Coe, H.: Vertical distribution of sub-micron aerosol chemical composition from North-Western Europe and the North-East Atlantic, Atmos. Chem. Phys., 9, 5389–5401, doi:10.5194/acp-9-5389-2009, 2009.

Morgan, W. T., Allan, J. D., Bower, K. N., Highwood, E. J., Liu, D., McMeeking, G. R., Northway, M. J., Williams, P. I., Krejci, R., and Coe, H.: Airborne measurements of the spatial distribution of aerosol chemical composition across Europe and evolution of the organic fraction, Atmos. Chem. Phys., 10, 4065–4083, doi:10.5194/acp-10-4065-2010, 2010.

ACPD
14, 25095–25138, 2014

Ng, N. L., Canagaratna, M. R., Zhang, Q., Jimenez, J. L., Tian, J., Ulbrich, I. M., Kroll, J. H., Docherty, K. S., Chhabra, P. S., Bahreini, R., Murphy, S. M., Seinfeld, J. H., Hildebrandt, L., Donahue, N. M., DeCarlo, P. F., Lanz, V. A., Prévôt, A. S. H., Dinar, E., Rudich, Y., and Worsnop, D. R.: Organic aerosol components observed in Northern Hemispheric datasets from Aerosol Mass Spectrometry, Atmos. Chem. Phys., 10, 4625–4641, doi:10.5194/acp-10-4625-2010, 2010.

Nowak, J. B., Neuman, J. A., Kozai, K., Huey, L. G., Tanner, D. J., Holloway, J. S., Ryerson, T. B., Frost, G. J., McKeen, S. A., and Fehsenfeld, F. C.: A chemical ionization mass spectrometry technique for airborne measurements of ammonia, J. Geophys. Res.-Atmos., 112, D10S02, doi:10.1029/2006jd007589, 2007.

O'Shea, S. J., Allen, G., Gallagher, M. W., Bauguitte, S. J.-B., Illingworth, S. M., Le Breton, M., Muller, J. B. A., Percival, C. J., Archibald, A. T., Oram, D. E., Parrington, M., Palmer, P. I., and Lewis, A. C.: Airborne observations of trace gases over boreal Canada during BORTAS: campaign climatology, air mass analysis and enhancement ratios, Atmos. Chem. Phys., 13, 12451–12467, doi:10.5194/acp-13-12451-2013, 2013a.

O'Shea, S. J., Bauguitte, S. J.-B., Gallagher, M. W., Lowry, D., and Percival, C. J.: Development of a cavity-enhanced absorption spectrometer for airborne measurements of CH_4 and CO_2, Atmos. Meas. Tech., 6, 1095–1109, doi:10.5194/amt-6-1095-2013, 2013b.

Palmer, P. I., Parrington, M., Lee, J. D., Lewis, A. C., Rickard, A. R., Bernath, P. F., Duck, T. J., Waugh, D. L., Tarasick, D. W., Andrews, S., Aruffo, E., Bailey, L. J., Barrett, E., Bauguitte, S. J.-B., Curry, K. R., Di Carlo, P., Chisholm, L., Dan, L., Forster, G., Franklin, J. E., Gibson, M. D., Griffin, D., Helmig, D., Hopkins, J. R., Hopper, J. T., Jenkin, M. E., Kindred, D., Kliever, J., Le Breton, M., Matthiesen, S., Maurice, M., Moller, S., Moore, D. P., Oram, D. E., O'Shea, S. J., Owen, R. C., Pagniello, C. M. L. S., Pawson, S., Percival, C. J., Pierce, J. R., Punjabi, S., Purvis, R. M., Remedios, J. J., Rotermund, K. M., Sakamoto, K. M., da Silva, A. M., Strawbridge, K. B., Strong, K., Taylor, J., Trigwell, R., Tereszchuk, K. A., Walker, K. A., Weaver, D., Whaley, C., and Young, J. C.: Quantifying the impact of BOReal forest fires on Tropospheric oxidants over the Atlantic using Aircraft and Satellites (BORTAS) experiment: design, execution and science overview, Atmos. Chem. Phys., 13, 6239–6261, doi:10.5194/acp-13-6239-2013, 2013.

Parrington, M., Palmer, P. I., Henze, D. K., Tarasick, D. W., Hyer, E. J., Owen, R. C., Helmig, D., Clerbaux, C., Bowman, K. W., Deeter, M. N., Barratt, E. M., Coheur, P.-F., Hurtmans, D., Jiang, Z., George, M., and Worden, J. R.: The influence of boreal biomass burning emissions

ACPD
14, 25095–25138, 2014

on the distribution of tropospheric ozone over North America and the North Atlantic during 2010, Atmos. Chem. Phys., 12, 2077–2098, doi:10.5194/acp-12-2077-2012, 2012.
Parrington, M., Palmer, P. I., Lewis, A. C., Lee, J. D., Rickard, A. R., Di Carlo, P., Taylor, J. W., Hopkins, J. R., Punjabi, S., Oram, D. E., Forster, G., Aruffo, E., Moller, S. J., Bauguitte, S. J.-B., Allan, J. D., Coe, H., and Leigh, R. J.: Ozone photochemistry in boreal biomass burning plumes, Atmos. Chem. Phys., 13, 7321–7341, doi:10.5194/acp-13-7321-2013, 2013.
Petzold, A., Weinzierl, B., Huntrieser, H., Stohl, A., Real, E., Cozic, J., Fiebig, M., Hendricks, J., Lauer, A., Law, K., Roiger, A., Schlager, H., and Weingartner, E.: Perturbation of the European free troposphere aerosol by North American forest fire plumes during the ICARTT-ITOP experiment in summer 2004, Atmos. Chem. Phys., 7, 5105–5127, doi:10.5194/acp-7-5105-2007, 2007.
Reid, J. S. and Hobbs, P. V.: Physical and optical properties of young smoke from individual biomass fires in Brazil, J. Geophys. Res.-Atmos., 103, 32013–32030, 1998.
Reid, J. S., Koppmann, R., Eck, T. F., and Eleuterio, D. P.: A review of biomass burning emissions part II: intensive physical properties of biomass burning particles, Atmos. Chem. Phys., 5, 799–825, doi:10.5194/acp-5-799-2005, 2005.
Schneider, J., Weimer, S., Drewnick, F., Borrmann, S., Helas, G., Gwaze, P., Schmid, O., Andreae, M. O., and Kirchner, U.: Mass spectrometric analysis and aerodynamic properties of various types of combustion-related aerosol particles, Int. J. Mass Spectrom., 258, 37–49, doi:10.1016/j.ijms.2006.07.008, 2006.
Schwarz, J. P., Gao, R. S., Fahey, D. W., Thomson, D. S., Watts, L. A., Wilson, J. C., Reeves, J. M., Darbeheshti, M.,. Baumgardner, D. G, Kok, G. L., Chung, S. H., Schulz, M., Hendricks, J., Lauer, A., Kärcher, B., Slowik, J. G., Rosenlof, K. H., Thompson, T. L., Langford, A. O., Loewenstein, M., and Aikin, K. C.: Single-particle measurements of midlatitude black carbon and light-scattering aerosols from the boundary layer to the lower stratosphere, J. Geophys. Res.-Atmos., 111, D16207, doi:10.1029/2006jd007076, 2006.
Simoneit, B. R. T., Schauer, J. J., Nolte, C. G., Oros, D. R., Elias, V. O., Fraser, M. P., Rogge, W. F., and Cass, G. R.: Levoglucosan, a tracer for cellulose in biomass burning and atmospheric particles, Atmos. Environ., 33, 173–182, doi:10.1016/s1352-2310(98)00145-9, 1999.
Sinha, P., Hobbs, P. V., Yokelson, R. J., Bertschi, I. T., Blake, D. R., Simpson, I. J., Gao, S., Kirchstetter, T. W., and Novakov, T.: Emissions of trace gases and particles from savanna

ACPD
14, 25095–25138, 2014

fires in southern Africa, J. Geophys. Res.-Atmos., 108, 8487, doi:10.1029/2002jd002325, 2003.

Slowik, J. G., Stroud, C., Bottenheim, J. W., Brickell, P. C., Chang, R. Y.-W., Liggio, J., Makar, P. A., Martin, R. V., Moran, M. D., Shantz, N. C., Sjostedt, S. J., van Donkelaar, A., Vlasenko, A., Wiebe, H. A., Xia, A. G., Zhang, J., Leaitch, W. R., and Abbatt, J. P. D.: Characterization of a large biogenic secondary organic aerosol event from eastern Canadian forests, Atmos. Chem. Phys., 10, 2825–2845, doi:10.5194/acp-10-2825-2010, 2010.

Sullivan, A. P., Holden, A. S., Patterson, L. A., McMeeking, G. R., Kreidenweis, S. M., Malm, W. C., Hao, W. M., Wold, C. E., and Collett Jr., J. L.: A method for smoke marker measurements and its potential application for determining the contribution of biomass burning from wildfires and prescribed fires to ambient $PM_{2.5}$ organic carbon, J. Geophys. Res.-Atmos., 113, D22302, doi:10.1029/2008jd010216, 2008.

Taylor, J. W., Allan, J. D., Allen, G., Coe, H., Williams, P. I., Flynn, M. J., Le Breton, M., Muller, J. B. A., Percival, C. J., Oram, D., Forster, G., Lee, J. D., Rickard, A. R., and Palmer, P. I.: Size-dependent wet removal of black carbon in Canadian biomass burning plumes, Atmos. Chem. Phys. Discuss., 14, 19469–19513, doi:10.5194/acpd-14-19469-2014, 2014.

Textor, C., Schulz, M., Guibert, S., Kinne, S., Balkanski, Y., Bauer, S., Berntsen, T., Berglen, T., Boucher, O., Chin, M., Dentener, F., Diehl, T., Easter, R., Feichter, H., Fillmore, D., Ghan, S., Ginoux, P., Gong, S., Grini, A., Hendricks, J., Horowitz, L., Huang, P., Isaksen, I., Iversen, I., Kloster, S., Koch, D., Kirkevåg, A., Kristjansson, J. E., Krol, M., Lauer, A., Lamarque, J. F., Liu, X., Montanaro, V., Myhre, G., Penner, J., Pitari, G., Reddy, S., Seland, Ø., Stier, P., Takemura, T., and Tie, X.: Analysis and quantification of the diversities of aerosol life cycles within AeroCom, Atmos. Chem. Phys., 6, 1777–1813, doi:10.5194/acp-6-1777-2006, 2006.

Vay, S. A., Choi, Y., Vadrevu, K. P., Blake, D. R., Tyler, S. C., Wisthaler, A., Hecobian, A., Kondo, Y., Diskin, G. S., Sachse, G. W., Woo, J.-H., Weinheimer, A. J., Burkhart, J. F., Stohl, A., and Wennberg, P. O.: Patterns of CO_2 and radiocarbon across high northern latitudes during International Polar Year 2008, J. Geophys. Res.-Atmos., 116, D14301, doi:10.1029/2011jd015643, 2011.

Warneke, C., de Gouw, J. A., Stohl, A., Cooper, O. R., Goldan, P. D., Kuster, W. C., Holloway, J. S., Williams, E. J., Lerner, B. M., McKeen, S. A., Trainer, M., Fehsenfeld, F. C., Atlas, E. L., Donnelly, S. G., Stroud, V., Lueb, A., and Kato, S.: Biomass burning and anthropogenic sources of CO over New England in the summer 2004, J. Geophys. Res.-Atmos., 111, D23S15, doi:10.1029/2005jd006878, 2006.

ACPD
14, 25095–25138, 2014

Weimer, S., Alfarra, M. R., Schreiber, D., Mohr, M., Prevot, A. S. H., and Baltensperger, U.: Organic aerosol mass spectral signatures from wood-burning emissions: influence of burning conditions and wood type, J. Geophys. Res.-Atmos., 113, D10304, doi:10.1029/2007jd009309, 2008.

Yokelson, R. J., Susott, R., Ward, D. E., Reardon, J., and Griffith, D. W. T.: Emissions from smoldering combustion of biomass measured by open-path Fourier transform infrared spectroscopy, J. Geophys. Res.-Atmos., 102, 18865–18877, doi:10.1029/97jd00852, 1997.

Yokelson, R. J., Urbanski, S. P., Atlas, E. L., Toohey, D. W., Alvarado, E. C., Crounse, J. D., Wennberg, P. O., Fisher, M. E., Wold, C. E., Campos, T. L., Adachi, K., Buseck, P. R., and Hao, W. M.: Emissions from forest fires near Mexico City, Atmos. Chem. Phys., 7, 5569–5584, doi:10.5194/acp-7-5569-2007, 2007.

Yokelson, R. J., Crounse, J. D., DeCarlo, P. F., Karl, T., Urbanski, S., Atlas, E., Campos, T., Shinozuka, Y., Kapustin, V., Clarke, A. D., Weinheimer, A., Knapp, D. J., Montzka, D. D., Holloway, J., Weibring, P., Flocke, F., Zheng, W., Toohey, D., Wennberg, P. O., Wiedinmyer, C., Mauldin, L., Fried, A., Richter, D., Walega, J., Jimenez, J. L., Adachi, K., Buseck, P. R., Hall, S. R., and Shetter, R.: Emissions from biomass burning in the Yucatan, Atmos. Chem. Phys., 9, 5785–5812, doi:10.5194/acp-9-5785-2009, 2009.

Zhang, Q., Worsnop, D. R., Canagaratna, M. R., and Jimenez, J. L.: Hydrocarbon-like and oxygenated organic aerosols in Pittsburgh: insights into sources and processes of organic aerosols, Atmos. Chem. Phys., 5, 3289–3311, doi:10.5194/acp-5-3289-2005, 2005.

Zhang, Q., Jimenez, J. L., Canagaratna, M. R., Allan, J. D., Coe, H., Ulbrich, I., Alfarra, M. R., Takami, A., Middlebrook, A. M., Sun, Y. L., Dzepina, K., Dunlea, E., Docherty, K., DeCarlo, P. F., Salcedo, D., Onasch, T., Jayne, J. T., Miyoshi, T., Shimono, A., Hatakeyama, S., Takegawa, N., Kondo, Y., Schneider, J., Drewnick, F., Borrmann, S., Weimer, S., Demerjian, K., Williams, P., Bower, K., Bahreini, R., Cottrell, L., Griffin, R. J., Rautiainen, J., Sun, J. Y., Zhang, Y. M., and Worsnop, D. R.: Ubiquity and dominance of oxygenated species in organic aerosols in anthropogenically-influenced Northern Hemisphere midlatitudes, Geophys. Res. Lett., 34, L13801, doi:10.1029/2007gl029979, 2007.

ACPD
14, 25095–25138, 2014

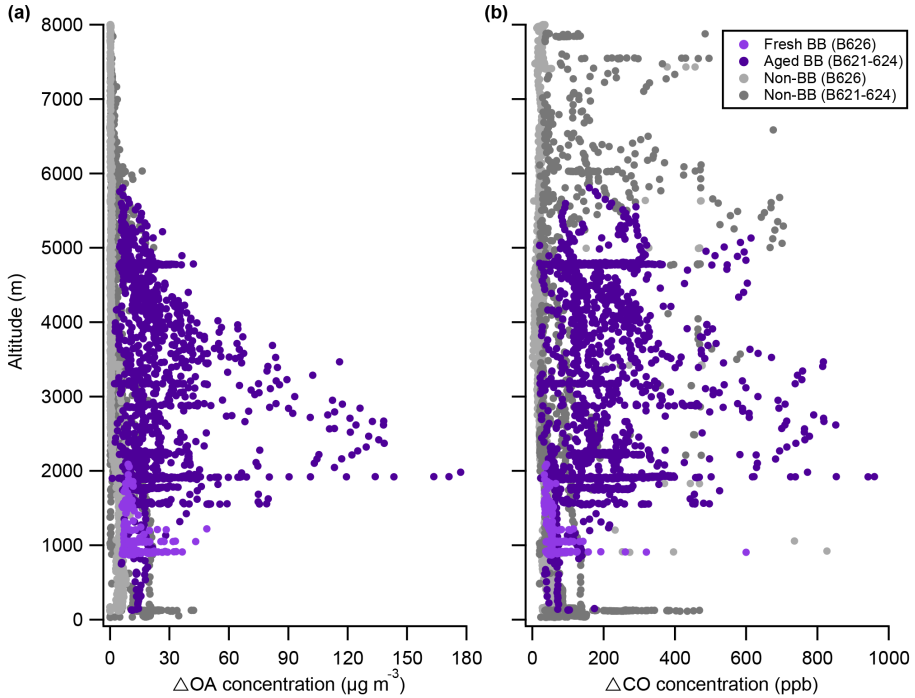

Figure 1. Vertical profiles of **(a)** ΔOA and **(b)** ΔCO in fresh and aged plumes, together with concentrations in air masses free from the influence of biomass burning.

ACPD
14, 25095–25138, 2014

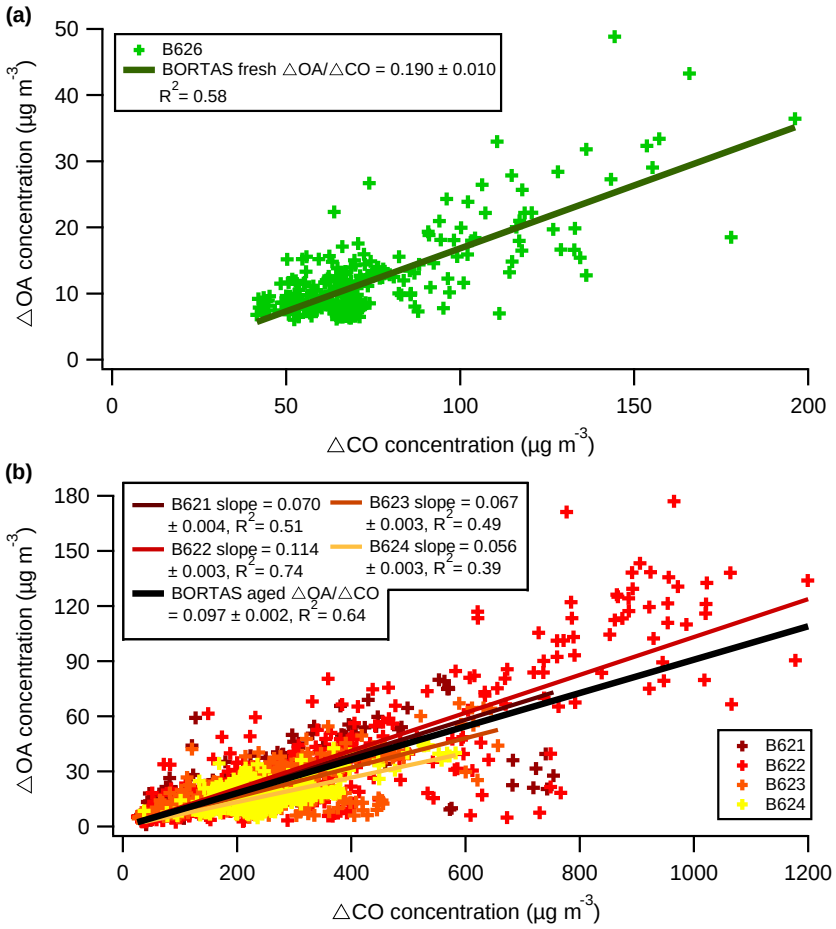

Figure 2. ΔOA vs. ΔCO for **(a)** fresh and **(b)** aged plumes. Coefficients are for linear regressions, from which average ΔOA/ΔCO ratios are derived, with uncertainties of ±1σ.

ACPD
14, 25095–25138, 2014

Properties and evolution of biomass burning organic aerosol

M. D. Jolleys et al.

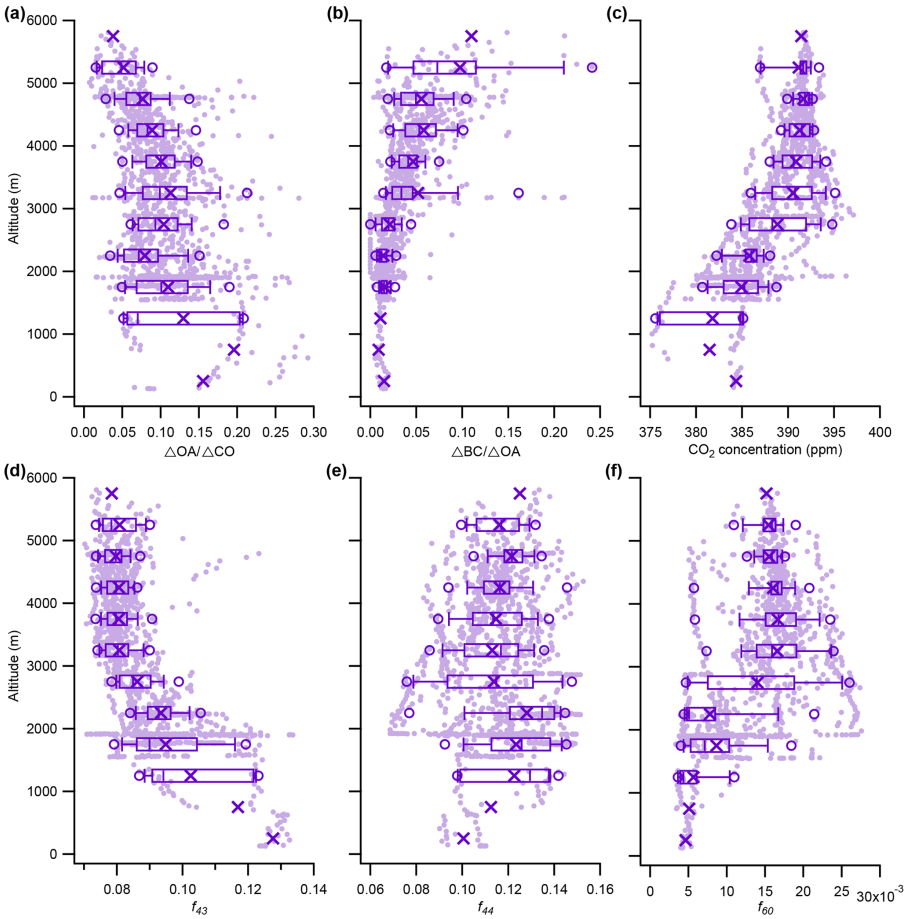

Figure 3. Vertical profiles of **(a)** ΔOA/ΔCO, **(b)** ΔBC/ΔOA, **(c)** CO_2, **(d)** f_{43}, **(e)** f_{44} and **(f)** f_{60} in aged plumes. Circles represent the 5th and 95th percentiles, vertical lines the 10th, 25th, 50th, 75th and 90th percentile, with crosses denoting mean values in each 500 m altitudinal bin.

ACPD
14, 25095–25138, 2014

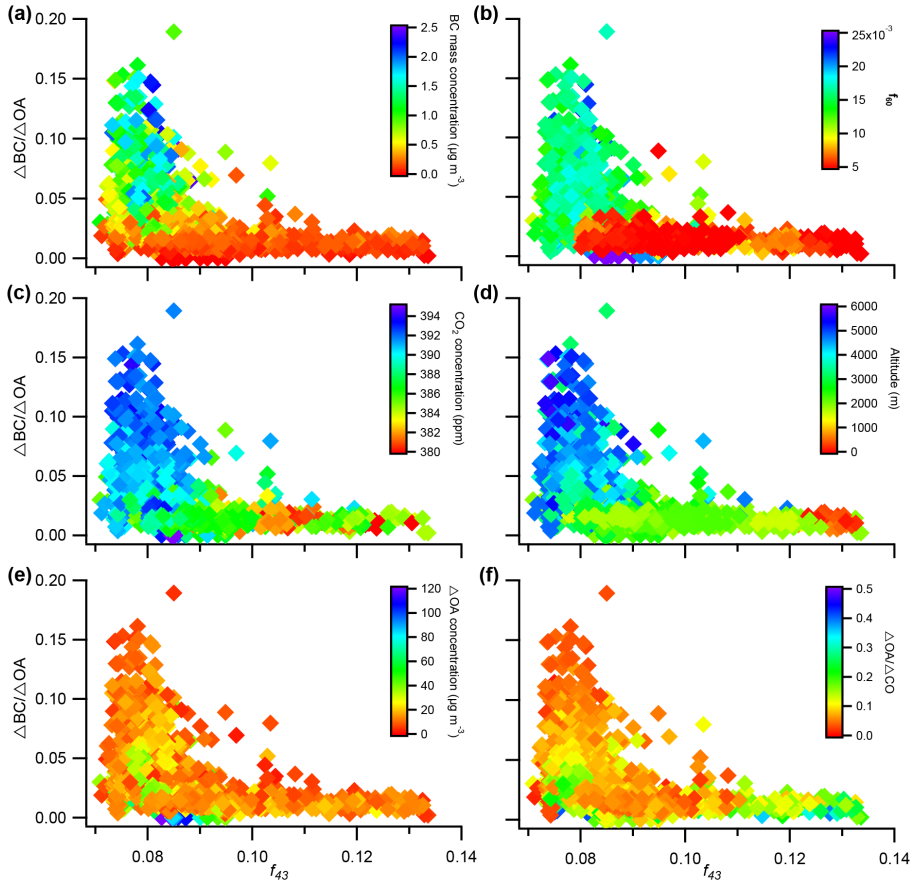

Figure 4. ΔBC/ΔOA vs. f_{43} for aged emissions. Datapoints are coloured to show relationships with **(a)** ΔBC, **(b)** f_{60}, **(c)** CO_2, **(d)** altitude, **(e)** ΔOA and **(f)** ΔOA/CO.

ACPD
14, 25095–25138, 2014

Properties and evolution of biomass burning organic aerosol

M. D. Jolleys et al.

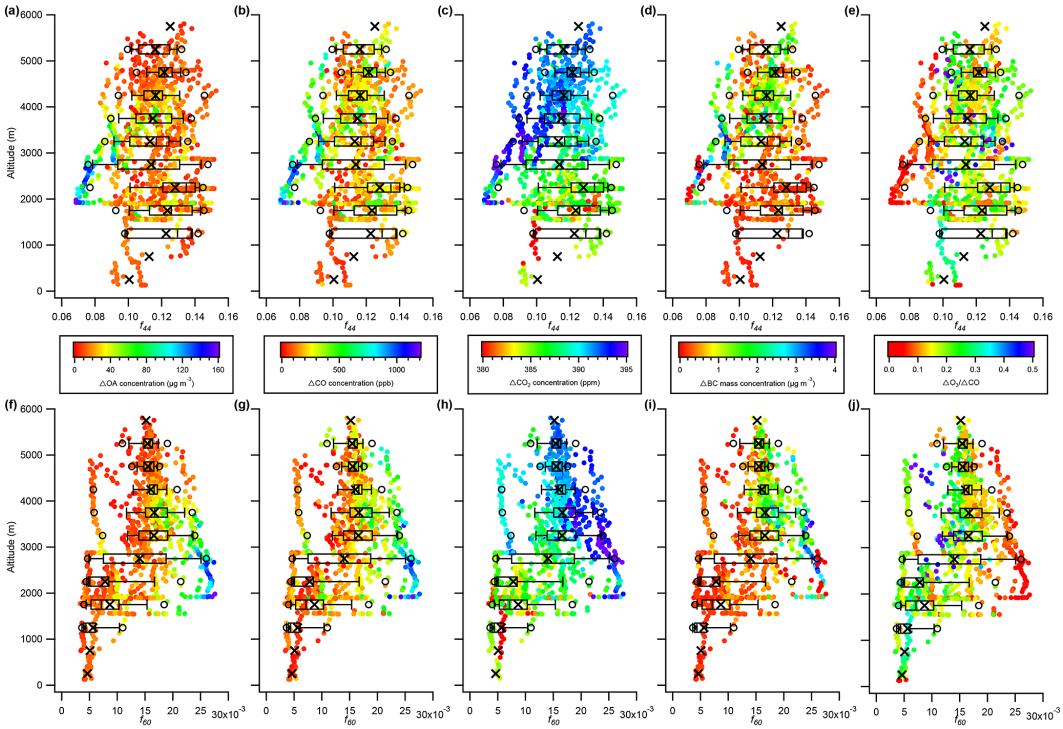

Figure 5. Vertical profiles of **(a–e)** f_{44} and **(f–j)** f_{60} in aged plumes. Datapoints are coloured by **(a, f)** ΔOA, **(b, g)** ΔCO, **(c, h)** CO_2, **(d, i)** ΔBC and **(e, j)** $\Delta O_3/\Delta CO$. Circles represent the 5th and 95th percentiles, vertical lines the 10th, 25th, 50th, 75th and 90th percentile, with crosses denoting mean values in each 500 m altitudinal bin.

ACPD
14, 25095–25138, 2014

Properties and evolution of biomass burning organic aerosol

M. D. Jolleys et al.

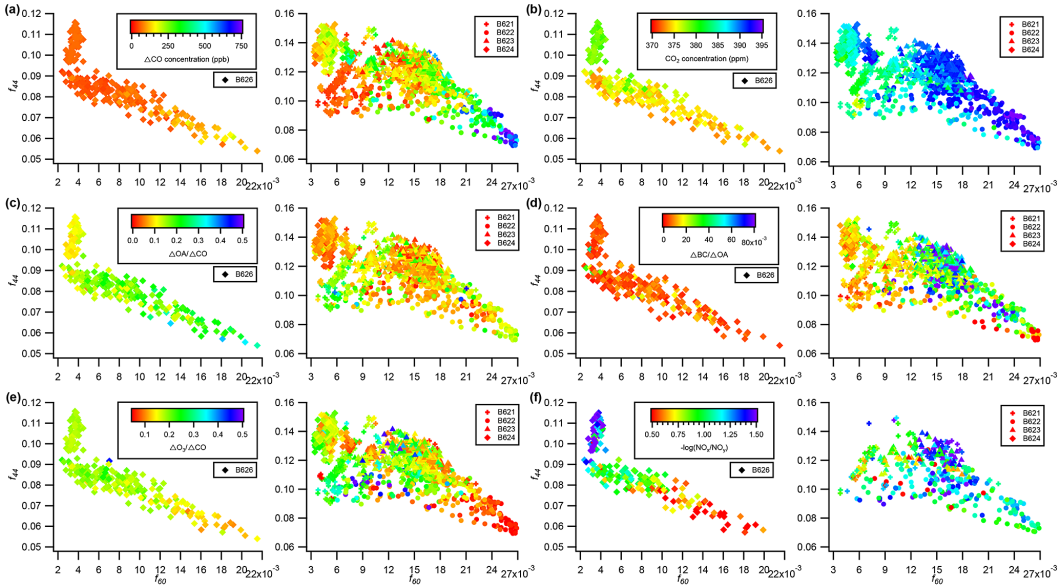

Figure 6. f_{44} vs. f_{60} with datapoints coloured by **(a)** ΔCO, **(b)** CO_2, **(c)** ΔOA/ΔCO, **(d)** ΔBC/ΔOA, **(e)** $\Delta O_3/\Delta CO$ and **(f)** $-\log(NO_x/NO_y)$. Data from fresh and aged plumes are shown on the left and right hand side of each panel, respectively.

ACPD
14, 25095–25138, 2014

Properties and evolution of biomass burning organic aerosol

M. D. Jolleys et al.

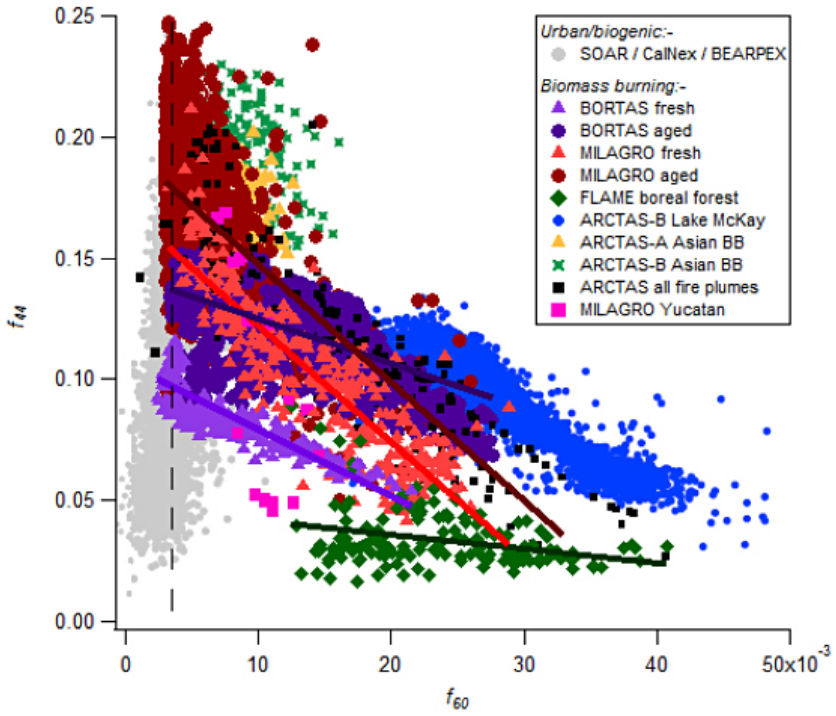

Figure 7. Synthesis of f_{44} vs. f_{60} from a range of ambient and laboratory measurements of BBOA, along with data from non-BB sources. The specified background f_{60} value of 0.003 used to identify BB influences is shown as the dashed vertical line. Coloured lines denote linear regressions for corresponding datasets. Adapted from Cubison et al. (2011).

ACPD
14, 25095–25138, 2014

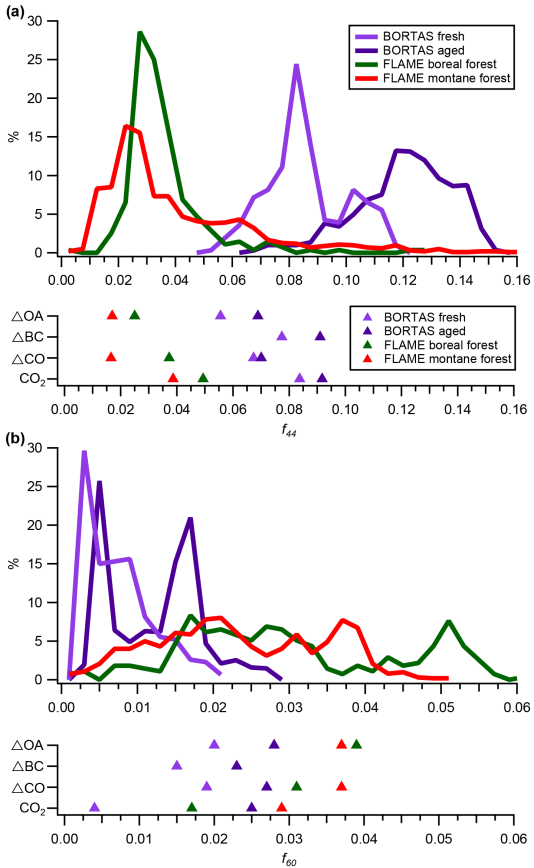

Figure 8. Probability density functions for **(a)** f_{44} and **(b)** f_{60} from a range of ambient and laboratory BB measurements. Also shown in the lower sections of each panel are the f_{44} and f_{60} values corresponding to maximum concentrations of ΔOA, ΔBC, ΔCO and CO_2.

ACPD
14, 25095–25138, 2014